



University
of Bremen



Postgraduate Program in Environmental Physics (PEP)
Institute of Environmental Physics (IUP)
University of Bremen

Master Thesis

**Horizontal variability of tropospheric NO₂ as
observed by a MAX-DOAS instrument in Bremen**

Author: Sandhya Gautam

Date of Birth: 27.06.1996

Matriculation Number: 3170224

Email: sandhya@uni-bremen.de

First Examiner: Dr. Andreas Richter

Second Examiner: Prof. Dr. Mihalis Vrekoussis

Supervisor: Dr. Andreas Richter

Acknowledgement

I wish to express my deep sense of gratitude to my supervisor Dr. Andreas Richter, who welcomed me in his group and made this work possible. His guidance throughout the journey motivated me in achieving this milestone. Without his support it would not have been possible.

Secondly, to the panel of examiners, I would like to acknowledge again to Dr. Andreas Richter and Prof. Dr. Mihalis Vrekoussis for their constructive comments and suggestions.

A special thanks to Bremen air quality monitoring stations (BLUES) and Bremen weather station (DWD) who provided the in-situ and meteorological measurements respectively.

Lastly, I would like to thank my family and friends for their continuous support and understanding during this research work.

Abstract

In this study, the horizontal variability of tropospheric NO₂ is investigated using ground based Multi Axis Differential Optical Absorption Spectroscopy (MAX-DOAS) measurements in Bremen. The study analyzed one year dataset (01.01.2020 to 31.12.2020) of ground based MAX-DOAS observations at an elevation angle of 1° under 24 different viewing azimuthal angles. In addition to MAX-DOAS data, in-situ (to make systematic comparison between MAX-DOAS and in-situ data) and meteorological measurements (to see dependency of NO₂ concentration with meteorological parameters) are also used in the analysis.

The cross section of NO₂ is temperature dependent and in order to correct that, temperature correction is introduced and applied to the differential slant column densities (DSCDs) of NO₂ obtained in the visible spectral range. The correction of azimuthal dependence on the light path for NO₂ and O₄ is discussed to see if the angular dependency is decreased. Although the correction for O₄ is imperfect, at least some improvements can be found in O₄. And for NO₂, the correction is performed to extract part coming from differences in concentrations and to remove the part coming from light path differences. Moreover, slant columns are converted to volume mixing ratios using O₄ measurements.

Diurnal and weekend effects of NO₂ depicts that highest concentration of NO₂ during weekdays are mainly attributed to traffic emissions, photolysis rate and inhomogeneous distribution of NO₂ around measurement site. MAX-DOAS retrievals have shown consistent seasonal variations in NO₂ with maximum concentration in summer and minimum in winter. The azimuthal dependence of path averaged NO₂ VMR is investigated suggesting wintertime maxima and summertime minima because of the lower mixing height and slower photolysis rate of NO₂ during winter.

Path averaged NO₂ VMR from MAX-DOAS and near surface NO₂ VMR from in-situ measurements are compared. Both independent sets of data (except some traffic stations from in-situ measurements) agree with higher winter values. Furthermore, the comparison shows higher weekdays values suggesting anthropogenic NO₂ emissions as a significant contributor.

Finally, the effect of wind speed and wind direction on NO₂ is also analyzed which suggest that most of the anthropogenic NO₂ VMR is lowest at high speed and coming from the south-west direction.

Table of Contents

Chapter 1	1
Introduction	1
Chapter 2	4
Chemistry of the Troposphere	4
2.1 Nitrogen oxides in the atmosphere.....	4
2.2 Oxygen dimer (O ₄).....	6
2.3 Water vapor (H ₂ O)	7
Chapter 3	8
Radiative transfer in the atmosphere	8
3.1 Absorption of radiation.....	8
3.2 Scattering effects	9
Chapter 4	12
Measurement Techniques / Approach	12
4.1 DOAS overview	12
4.2 MAX-DOAS Instrument.....	13
4.3 Choice of reference spectrum.....	14
4.4 MAX-DOAS measurement setup.....	15
4.5 Zenith sky and Off-axis measurements	16
4.6 Azimuthal viewing directions	17
4.7 Differential slant column density	18
Chapter 5	19
Ancillary Measurements	19
5.1 Surface In-situ measurements of NO ₂ concentrations	19
5.2 Meteorological measurements	19
Chapter 6	20
Results and Discussions	20
6.1 Temperature correction of NO ₂ DSCDs	20
6.2 Directional correction of NO ₂ SCDs	21
6.3 Diurnal and weekend effects.....	24

6.4 Seasonal trends of NO ₂ , O ₄ and H ₂ O	27
6.5 Retrieval of path averaged near surface VMRs from MAXDOAS SCDs	28
6.6 Azimuthal dependence of path averaged NO ₂ VMR.....	30
6.7 Variation of In-situ NO ₂ measurements over different stations of Bremen.....	31
6.8 Comparison of MAX-DOAS data with In-situ measurements.....	35
6.9 Dependence of NO ₂ pollution levels on meteorological parameters.....	37
Chapter 7	40
Summary and Conclusions	40
References	43

Chapter 1

Introduction

The trace gases in the atmosphere have their own significant role; most of them contribute to air pollution. Among the group of the gaseous air pollutants, nitrogen dioxide (NO₂) acts as a very reactive trace gas in the atmosphere, especially in the troposphere and stratosphere. In this thesis, the focus is on the troposphere. NO₂ is usually emitted in the form of NO from human activities such as industry, fossil fuel combustion, transportation, and power plants.

Nitrogen oxide (NO_x, calculated as NO₂) emissions according to source categories.

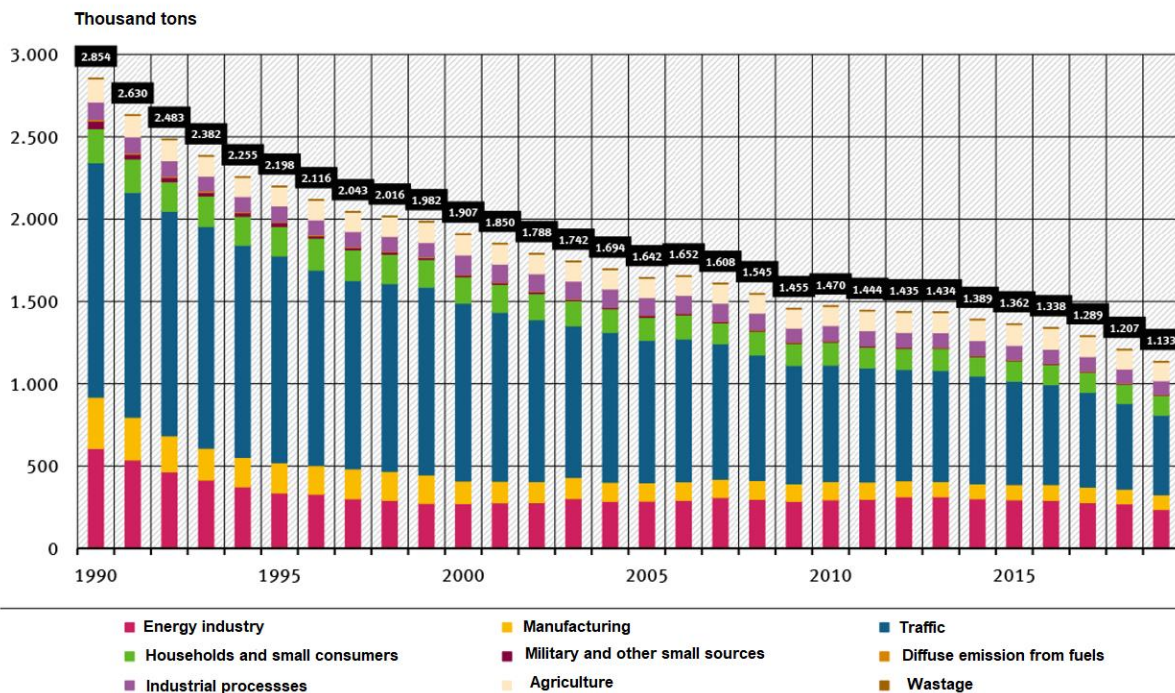


Figure 1. Nitrogen oxide (NO_x, calculated as NO₂) emissions according to source categories in Germany (Adapted from: The Federal Environment Agency, 2020).

The total NO₂ pollution continues to decline throughout Germany as can be seen in Figure 1. This arose because of strict environmental legislation, use of catalytic converters and use of cleaner fuels such as natural gas. Despite the reduction, the transport sector remains by far the

largest emitter of NO₂ from 1990 to 2018 (around 43%) followed by power plants and industrial processes. Households and small consumers such as heating system have the lowest specific emissions (The Federal Environment Agency, 2020). This kind of downward trend in NO₂ is found in many countries but not in countries with rapidly developing economies such as India or the Arabian countries (Georgoulas et al., 2019).

Measurements of NO₂ can be performed by either in-situ or remote sensing methods. The Multi Axis Differential Optical Absorption Spectroscopy (MAX-DOAS) technique (ground-based) is a commonly used technique for measuring a wide range of atmospheric trace gases. Because of the strong and well-defined absorption bands in the UV and visible spectral ranges, NO₂ molecule is an excellent target gas for retrievals deploying DOAS (Richter, 2009). It uses observation of scattered sunlight at several elevation angles between horizon and zenith (Irie et al., 2011). In this thesis, the horizontal variability of tropospheric NO₂ is investigated at a single elevation angle (1°) with multiple azimuthal observation directions under different conditions such as time, season, viewing direction, and meteorological conditions.

Since air pollution is one of the main environmental issues today, a number of studies have been conducted with the aim of describing and quantifying the trace gases. Several research on air pollution have been carried out in Bremen during the previous few decades (Blechschmidt et al., 2020, Bösch, 2018). Considering this, main motivation for the ongoing thesis is to investigate where the pollution comes from. To know the particular region, it is important to track back the sources of the pollution. One can trace high NO₂ observations back to a power plant using, for example, the wind direction and wind speed coming from the power plant. However, that is not simple because many sources like power plants, highways, and industries emit NO₂ which does not disappear from the air so quickly. Thus, what is noticed in the atmosphere is the fusion of the fresh and old emissions. In principle, under these circumstances, it would be interesting to understand the spatial distribution to be able to localize and track the sources back.

An additional motivation for the present work is it is challenging to compare the ground-based measurements and satellite data because the ground measurements are local, while satellite measurements cover a large area. The satellite providing the best spatial resolution for the detection of NO₂ so far is TROPOMI on Sentinel 5P, has the spatial resolution of about 3.5 km x 5.5 km (Smedt, et.al., 2021). If this spatial resolution is plotted on the map of Bremen, then it is clear that it covers, for example, power plants, the Bürgerpark, the highway, the city center, and

the industrial area. Satellite measurements are in any case not comparable with the one measurement that was taken at the University of Bremen for the same reason as explained in the starting of this paragraph. But if one wants to compare, then it becomes important how large the gradient or variation of NO_2 is around these measurements.

The framework of this thesis is as follows: Chapter 2 describes the chemistry of the troposphere focusing mainly on Nitrogen oxides, oxygen dimer and water vapor. Chapter 3 introduces radiative transfer in the atmosphere (absorption and scattering). Chapter 4 follows by the Differential Optical Absorption Spectroscopy (DOAS) technique and MAX-DOAS instrument setup along with the description of zenith sky and off-axis measurements followed by azimuthal viewing directions. The measurements used in the analysis in addition to MAX-DOAS measurements are described in Chapter 5 while Chapter 6 presents the results of the time series measurements (weekend, monthly and seasonal trend), comparison of MAX-DOAS measurements with in-situ data and variation of NO_2 pollution levels with meteorological parameters. Finally, Chapter 7 summarizes the main conclusion of this study.

Chapter 2

Chemistry of the Troposphere

The troposphere, lowest layer of the Earth's atmosphere has the average height of 0-10 km above the Earth's surface. This layer is primarily composed of Nitrogen (78%), Oxygen (21%) and a small fraction of Argon and other gases. The Earth's atmosphere contains less than 1% trace gases by volume. Several anthropogenic trace gases that have accumulated in the Earth's atmosphere could trigger future global warming or stratospheric ozone depletion and individually, higher concentrations of trace gases may add to the Earth's natural greenhouse effect (Rasmussen, et. al., 1985).

CO₂ is the most common trace gas, followed by He, CH₄, O₄, H₂O, and so on. Trace gases are found in small concentrations, yet they are vital for atmospheric chemistry, the Greenhouse gas effect, filtering of UV before it reaches the surface, and eventually, they are responsible for pollution. Spectroscopic methods are used to observe many of the trace gases in the atmosphere, which either absorb or scatter solar radiation. This chapter covers all of the trace gases observed during the research.

2.1 Nitrogen oxides in the atmosphere

Nitric oxide (NO) and nitrogen dioxide (NO₂) are the two nitrogen oxides (NO_x = NO + NO₂) that are relevant for air pollution since NO₂ and NO rapidly convert into each other in the atmosphere.

Sources

NO₂, emitted to the troposphere mostly in the form of NO originates from both natural and anthropogenic emissions such as microbiological processes in the soil, lightning, transportation, energy production and most dominant fossil fuel combustion. NO₂ is a key species in the tropospheric ozone formation and leads to the formation of HNO₃ and thus acid rain, which ultimately contributes to eutrophication.

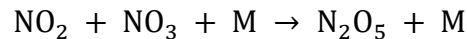
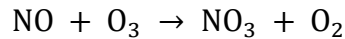
Sinks

During the day, removal of NO₂ from the atmosphere occurs mainly by reaction with OH, which forms nitric acid (M = N₂ or M = O₂).



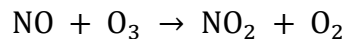
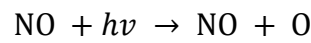
Nitric acid formed is mixed with clouds and aerosols and forms nitrate aerosols. This leads to the acidification of the aerosols and this nitric acid is removed from the atmosphere mainly by wet (acid rain) and dry deposition which subsequently affects the ecosystem (Finlayson-Pitts and Pitts, 2000).

Nitrogen oxide is converted to nitrate by reacting with ozone at night, while nitrogen dioxide is converted to dinitrogen pentoxide by reacting with nitrate.



Nitrate (NO_3) and dinitrogen pentoxide (N_2O_5) are removed by wet deposition from the atmosphere.

When discussing NO_2 in the atmosphere, it's necessary to understand the Leighton equilibrium, which describes the relationship between NO_2 , NO , and O_3 in the background atmosphere when volatile organic molecules are absent (VOCs).



Since NO_2 has a relatively short atmospheric lifetime (a few hours), it acts as a fresh pollutant and is characterized by large spatial and temporal variability. The concentration of most air pollutants is affected by meteorological conditions such as wind speed, wind direction and solar radiation which can worsen or improve the air quality depending on the nature of respective conditions. Low wind speed can cause high concentration of air pollution and vice versa. However, strong wind can transport pollution from other regions. During the summer season less NO_2 can be found due to the photolysis, although NO_x ($\text{NO} + \text{NO}_2$) remains the same, only the balance between NO and NO_2 is shifted. During the winter season, when there is less light, the lifetime of NO_2 will be longer due to the following two effects:

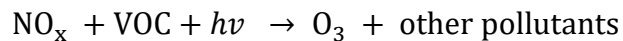
1. Photolysis changes the ratio between NO and NO_2 as described above.

2. The main sink of NO₂ is the reaction with OH (formed by photolysis), which results in less OH in winter than in summer. Because there is less OH in winter, the lifetime of NO₂ increases.

Therefore, the NO₂ concentration is higher in winter than in summer. Depending on the altitude, the mean tropospheric life time of NO_x varies from a few hours in summer to a few days in winter (Seyler et al., 2017).

Extensive research (Chan et.al., 2020) has been carried out to study the typical diurnal variation of NO₂ in the troposphere and it became apparent that concentration of NO₂ has an inverse relation with solar radiation. The NO₂ concentration is high during night time and as soon as the sun rises, it drops to about half of its original concentration due to the photolysis process. Therefore, a strong diurnal variation with low values of NO₂ in the morning and higher values in the evening is expected. Photolysis is not only the reason for the diurnal variation of NO₂ but the emissions from transportation during morning and evening rush hour, diurnal changes of the emission from power plants, and industries are also equally liable for this variation.

It is a well-known fact that tropospheric ozone is a pollutant. High ozone concentrations in the troposphere are formed when NO_x reacts with VOCs in presence of sunlight to form the secondary pollutant ozone (O₃) (Finlayson-Pitts and Pitts, 2000).



This ozone formation leads to photochemical smog which has a hazardous effect to human health and causes serious respiratory problems. The rate of this smog increases during summer months when the solar radiation and temperatures are higher.

2.2 Oxygen dimer (O₄)

The oxygen dimer (O₄) is the collision complex of two oxygen molecules (O₂) which has various absorption bands in the near ultraviolet (UV), visible (VIS) and near infrared (IR) and it absorbs weakly under clear sky conditions. (Gratsea et al., 2016).

The amount of NO₂ measured by MAX-DOAS depends on the NO₂ concentration in the atmosphere and the length of the light path. This can be considered by analyzing absorption of oxygen dimer (O₂ - O₂) in the MAX-DOAS data, since the oxygen concentration is known and any changes in measured O₄ results from a change in light path. Reasons for changes in light path are

changes in aerosol extinction in the lower troposphere as well as changes in the position of the Sun and viewing direction (Irie et al., 2011). O₄ observations help to yield information on the phase function of aerosol scattering at different azimuth angles (Wagner et. al., 2004).

2.3 Water vapor (H₂O)

Water vapor (H₂O) is an important natural greenhouse gas in the atmosphere, making life on Earth possible. However, in this work, it is used as a passive tracer to determine the length of the light path. The concentration of H₂O is dominated by the weather and is constant around the measurement location in first approximation. It has a weak absorption band in the visible spectral range while it is stronger in the near-infrared region. The retrieval of water vapor using DOAS depends on the absorption of solar radiation by atmospheric water vapor. Because of the possibility of phase transitions between solid, liquid, and gas phases, water vapor performs a unique role in the atmosphere.

Chapter 3

Radiative transfer in the atmosphere

The physical phenomenon of energy transmission in the form of electromagnetic radiation is known as radiative transfer. Solar radiation entering the atmosphere can be reflected back to space (clouds are important in this mechanism), transmitted to the surface (where it might be absorbed or reflected), or scattered by one of numerous atmospheric elements (that can be either in gaseous, liquid or solid phase). This chapter mainly discuss about the absorption (transfer of electromagnetic energy to another form e.g., heat by absorbing radiation) and scattering processes (direction of propagation of a photon and energy is changed).

3.1 Absorption of radiation

Atmospheric molecules (such as ozone, oxygen, nitrogen dioxide, or water vapor) or aerosols (such as soot) absorb radiation and causes extinction by Rayleigh and Mie scattering (Platt, et al., 2008). The basic quantity measured is the amount of trace gases in the atmosphere and the underlying hypothesis for measuring many quantitative trace gases analytically in the atmosphere and laboratory is Lambert - Beer's law.

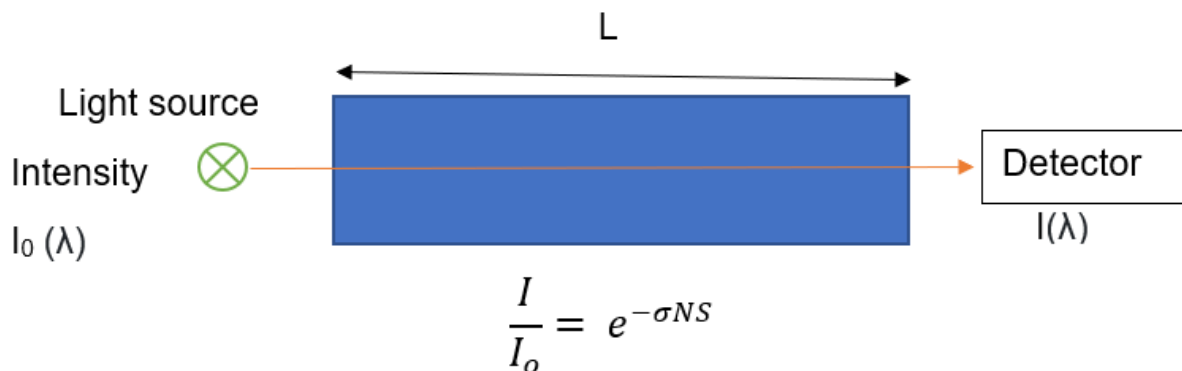


Figure 2. The absorption spectroscopic trace gas detection principle. (Adapted from Platt, et al., 2008)

A light beam with an initial intensity (I_0) passes through the absorbing medium of length L and the intensity (I) is measured by an appropriate detector at the end of the light path (see Figure 2). Lambert - Beer's law describes the intensity of light at a particular wavelength decreases exponentially in a uniform medium. After passing through an absorbing layer of thickness ds , the radiance will be lowered by the amount dI :

$$dI(\lambda) = -\rho\sigma(\lambda)I(\lambda)ds \quad (1)$$

with ρ being the concentration of absorbing molecules per volume and $\sigma(\lambda)$ the absorption cross section of an absorber. $I(\lambda)$ on the right side of the equation is the radiance.

Integration of equation (1) yields:

$$\ln\left(\frac{I_0(\lambda)}{I(\lambda)}\right) = -\sigma(\lambda)\int_0^L \rho ds \quad (2)$$

Where, L denotes the length of the light path. Thus, after passing through the absorbing layer, the radiance (equation 2) becomes:

$$I(\lambda) = I_0 e^{-\sigma(\lambda)\rho l} \quad (3)$$

Equation (4) gives radiation of intensity with distance and also known as Beer – Lambert's equation. In this work, the NO_2 absorption spectrum is retrieved in the wavelength region of 425-490 nm.

Also, from equation (2)

$$SC = \int_0^L \rho ds \quad (4)$$

is considered as the slant column density of the absorber.

3.2 Scattering effects

Mainly two types of scattering exist in the atmosphere; elastic or inelastic. Elastic scattering includes Rayleigh and Mie scattering while inelastic scattering can be described by Raman scattering / Ring effect.

Rayleigh Scattering

Rayleigh scattering takes place on air molecules which are small relative to the wavelength of visible light. Typically, molecules of N_2 or O_2 are the examples of such scattering for visible light.

This scattering is an elastic scattering because the energy of the scattered photons remains constant. Rayleigh scattering has a strong wavelength dependence which enhances the short wavelengths resulting the blue color of the sky. The scattering cross section is inversely proportional to the fourth power of wavelength and given as:

$$\sigma(\lambda) \propto \lambda^{-4} \quad (5)$$

And the phase function of Rayleigh scattering is given by (Sweigart,1969):

$$\phi(\cos \theta) = \frac{3}{4}(1 + \cos^2(\theta)) \quad (6)$$

where θ is the angle between the incident and scattering directions.

Mie Scattering

Gustav Mie was the first to explain Mie scattering in detail, and it is defined as the interaction of the light with particulate materials having dimensions similar or larger than the incident radiation's wavelength (Mie,1908). Mie scattering takes place on those particles which are large relative to the wavelength such as aerosols, cloud droplets or small water droplets. In contrast to Rayleigh scattering, this type of scattering has a less wavelength dependence (typically proportional to $\lambda^{-1.3}$). The Mie scattering cross section is complicated to determine but depending on the size and composition of the absorber simple type of polynomial dependency can be found.

$$\sigma(\lambda) \propto \lambda^{-1..+1} \quad (7)$$

The aerosol size parameter α determines the scattering phase function, which controls the direction and strength of scattered light:

$$\alpha = \frac{2\pi r}{\lambda} \quad (8)$$

with r as the radius of the aerosols and λ being the wavelength of the light.

Raman Scattering

Raman scattering is the inelastic scattering of photons by air molecules, resulting in an energy exchange as well as a change in the direction of the light. The contribution of inelastically scattered light to overall intensity causes a change that can be characterized as filling in of the Fraunhofer lines, complicating the complete removal of the Fraunhofer structures in DOAS retrieval: this effect is commonly referred to as the Ring effect (Wagner, et al., 2001). Rotational Raman scattering accounts for the majority of inelastic scattering in the atmosphere.

Chapter 4

Measurement Techniques / Approach

Trace gas composition in the atmosphere can be detected using remote sensing techniques at a distance from the probing equipment. In the present study, ground based remote sensing technique i.e., DOAS method has been used to account atmospheric trace gases.

4.1 DOAS overview

DOAS is a widely used inversion method for retrieving atmospheric trace gas abundances from multi-wavelength light measurements. When atmospheric trace gases were monitoring using an artificial light source, Platt et al. 1979, introduced this technique. The term DOAS reveals a lot about what it's all about: It's about 'Optical' measurements of light ranging from ultraviolet to visible to infrared part of electromagnetic spectrum. 'Absorption' describes the removal of light from incoming light of specific wavelengths, absorption and scattering of molecules. 'Spectroscopy' is defined as the interaction of light with matter. Finally, 'Differential' indicates that the change in signal with wavelength rather than absolute signal is being analyzed.

DOAS can be divided into active and passive types based on their light sources. Active DOAS makes use of artificial light e.g., Xe-arc lamps and average surface concentrations of trace gases are retrieved (Zhou, et. al., 2009) whereas passive DOAS uses natural light sources such as the sun, moon, or stars. Initially, the DOAS method was applied to quantify tropospheric gases e.g., NO₂, using active DOAS. However, a few years later DOAS was additionally applied as passive DOAS (i.e., using direct and scattered sunlight observations) (Schreier et al., 2020). Many atmospheric trace gases can be measured using DOAS techniques, such as O₃, NO₂, HONO, SO₂, BrO, IO, and OCIO, in addition to 30 kinds of hydrocarbons (Vandaele et al., 2005).

The basic principle used in DOAS is absorption spectroscopy. Light travelling through the atmosphere is partly absorbed by trace constituents along the way following Lambert Beer's law of absorption (see equation 3). In the real atmosphere, a number of absorbers are present instead of one. Therefore, the effects of all these absorbers should be taken into account and this can be proceeded by adding absorption of trace gases. Each molecule has a characteristic absorption spectrum i.e., different strength of spectrum and specific wavelength dependency. Adding the effect of multiple absorbers in equation 3 gives:

$$I(\lambda) = I_0(\lambda) \exp\left\{-\sum_{i=1}^N \sigma(\lambda)\rho l - \sigma_{Ray}(\lambda)\rho_{Ray}l - \sigma_{Mie}(\lambda)\rho_{Mie}l\right\} \quad (9)$$

With N being the number of absorbing species.

Using equation 4 in above equation results:

$$I(\lambda) = I_0(\lambda) \exp\left\{-\sum_{i=1}^N \sigma_i(\lambda)SC_i - \sigma_{Ray}(\lambda)SC_{Ray} - \sigma_{Mie}(\lambda)SC_{Mie}\right\} \quad (10)$$

DOAS technique is all about removing the scattering effects from the measurements. In that context, Rayleigh and Mie scattering cross sections can be expressed as polynomials of some coefficients. Now, equation 10 transforms into:

$$I(\lambda) = I_0(\lambda) \exp\left\{-\sum_{i=1}^N \sigma_i(\lambda)SC_i - \sum_{j=0}^M p\lambda^j\right\} \quad (11)$$

Taking natural logarithm of equation 11 yields:

$$\ln \frac{I(\lambda)}{I_0(\lambda)} = -\sum_{i=1}^N \sigma_i(\lambda)SC_i + \sum_{j=0}^M p\lambda^j \quad (12)$$

Equation 12 is so called DOAS equation. The right side of equation 12 is the sum of all absorptions which is the product of absorption cross section of the molecule and the slant column of the absorber (this quantity will be determined later in this study) and the polynomial is there to compensate the scattering effect.

4.2 MAX-DOAS Instrument

A passive remote sensing technique named Multi Axis Differential Optical Absorption Spectroscopy (MAX-DOAS) technique is applied to retrieve / detect trace gases under different elevation angles and viewing directions. In ground-based MAX-DOAS measurements, the sensitivity to absorbers in the lower few kilometers of the atmosphere is large and vertical profiles can be determined using Radiative transfer Model (RTM) calculations (Hönninger et al., 2004). Traditionally, instrument setups were pointed exclusively to the zenith and were mainly sensitive to stratospheric trace gases. However, this measurement technique was further developed in order

to enhance the sensitivity towards trace gases which are closer to the surface. This thesis presents measurements performed with a ground-based MAX-DOAS instrument.



Figure 3. The MAX-DOAS telescope units as installed on the roof of the IUP Bremen. The closed telescope box is looking above horizon (left panel) and the inside of the telescope box (right panel).

MAX-DOAS devices are suitable for carrying out long term measurements and have also been installed on different platforms such as airplanes, cars and ships. Several applications are currently using MAX-DOAS, including assessing volcanic plumes (SO_2 , BrO), natural emissions of trace gases, etc. In contrast to active DOAS, MAX-DOAS instrument can be used during daylight hours.

4.3 Choice of reference spectrum

A ground-based instrument cannot measure an extraterrestrial spectrum $I_0(\lambda)$, which is a complication. A zenith measurement is commonly employed as a reference, but other viewing angles are also suitable for reference spectrum. While choosing reference spectrum, one should pick those measurements which has low absorption (less sensitivity) as possible. For off-axis measurement, the smaller the elevation angle, the higher is the sensitivity in the boundary layer. Due to this, zenith measurements are chosen for the reference spectrum.

Assuming that there is only one absorber present and ignoring scattering terms, logarithm of equation 4 (using equation 3) gives:

$$\ln \frac{I}{I_0} = -\sigma SC$$

Since, MAX-DOAS is unable to measure $I_0(\lambda)$, a measurement of $\frac{I}{I_{ref}}$ can be made instead of $\frac{I}{I_0}$.

$$\ln\left(\frac{I}{I_{ref}}\right) = \ln\left(\frac{I}{I_0}\right) - \ln\left(\frac{I_{ref}}{I_0}\right)$$

$$\ln\left(\frac{I}{I_{ref}}\right) = -\sigma(SC - SC_{ref})$$

4.4 MAX-DOAS measurement setup

The measurements were performed from 1st January 2020 to 31st December 2020. During the measurements the MAX-DOAS instrument was set up on the roof of the Institute of Environmental Physics (IUP) Bremen. The instrument consists of a pointable telescope collecting the scattered light, a grating spectrometer for the separation into wavelengths and a CCD detector for the measurement of the spectrum. The telescope is located on the roof of the building and is connected to the spectrometer in the lab via a quartz fibre bundle. Calibration measurements are automatically performed every day. The scattered solar light is collected by the telescope sent to the spectrometer for spectrum analysis via quartz fibre bundles and the detector records the spectra, which is then saved on computer that controls the entire setup. (Wittrock, et al., 2004).

Telescope unit

The telescope housing of the MAX-DOAS instrument is positioned on a pan-and-tilt head that allows direct aiming in any viewing direction. The telescope has a single viewing port that does not have a mirror. It is pointed in the sky at various angles to collect scattered sunlight. Figure 3 (right panel) shows the telescope unit with its parts.

Charge Coupled device Detector (CCD)

This detector is used to convert the spectrum first into electrical charges and then digital signals which are analyzed by the computer.

Quartz fibre bundle

The collected light travels through the quartz fibre bundle to the spectrometer.

Grating Spectrometer

Grating is a dispersive element which works using multibeam interference. The spectrometer separates the different wavelengths contained in the incoming light. The spectrometer used in this study is of the Czerny Turner type.

The observed spectra of scattered sunlight were analyzed by using DOAS algorithm (Platt, 1994). The slant column density (SCD) of the trace gases is determined first using respective algorithm. The offset and dark current of all measured spectra were corrected first and the off-axis measurement is then divided by the corresponding zenith reference spectrum, then converted to optical density using the logarithm function (Tan, et al., 2019). A nonlinear least square fitting technique is used to fit several trace gas absorption cross sections, as well as a Fraunhofer reference spectra, a Ring spectrum, and a polynomial (order 4, for Rayleigh scattering) into the spectral fitting process in order to retrieve differential slant column densities (DSCDs). The software used for the spectral analysis is NLIN_D program using the DOAS equation (equation 12).

4.5 Zenith sky and Off-axis measurements

When the instrument measures the scattered sunlight not looking into the sun but straight into the sky, such measurements are called zenith sky measurements. Because of the geometry of zenith direction, the solar radiation travels a longer path through the stratosphere and a shorter path through the troposphere. The zenith sky geometry provides low sensitivity for the tropospheric measurements and is therefore used as a background measurement. Twilight measurements are convenient for stratospheric observations only if one is interested, for example, in the chemistry of the ozone layer.

To measure absorption near the ground in the boundary layer, where the pollution is greatest, off-axis measurements are proving practical. The basic idea is that the viewing directions with small elevation angles have a very long light path in the lowest atmospheric layers while the light path in the upper troposphere and stratosphere does not depend strongly on the viewing direction. It is clearly seen from Figure 4 that as the elevation angle decreases, the light path in the boundary layer increases.

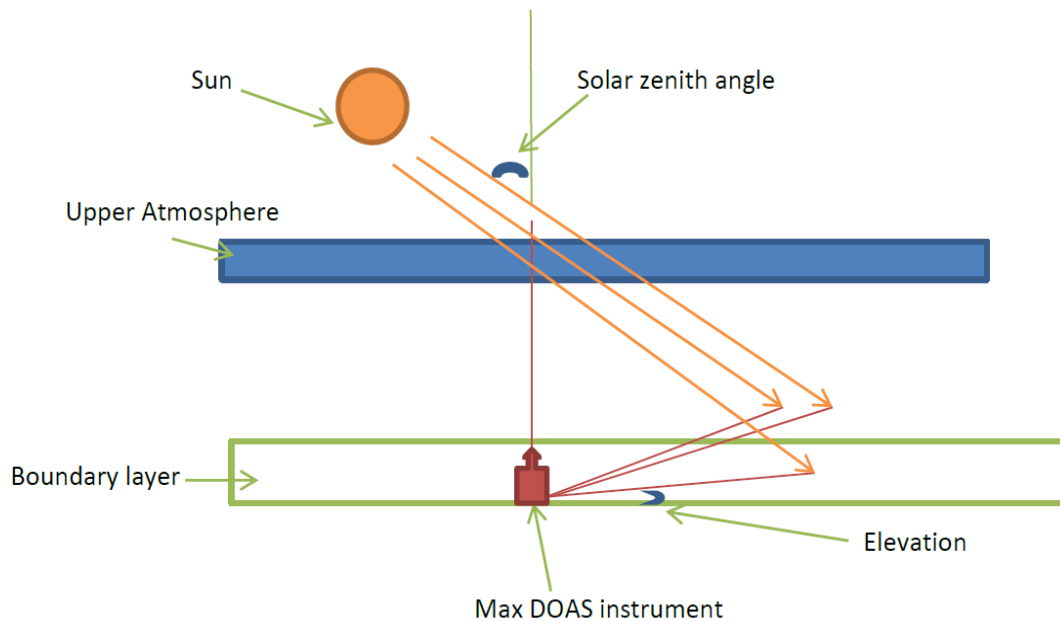


Figure 4. The looking direction of the telescope into different atmospheric layers and the light paths for scattered light observations.

4.6 Azimuthal viewing directions

The idea is to measure the variability of NO_2 around the institute, and therefore the instrument takes measurements at different azimuth angles ranging from 130° to 360° with a difference of 10° between each measured angle. The respective angles start from north in an anticlockwise direction. The viewing azimuth is the horizontal direction in which the instrument is looking, where 0° is north, 90° is east, 180° is south, and 270° is west. The elevation angle used in this study is the lowest one (1°).

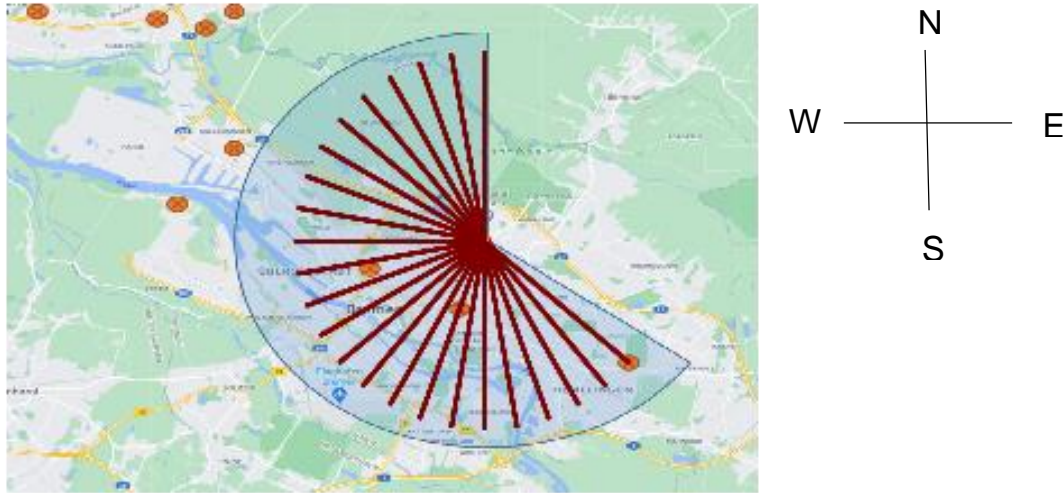


Figure 5. Viewing azimuth directions (maroon color lines) of the MAX-DOAS instrument in IUP Bremen. The circled cross shows the geographical position of the in-situ instruments which are used in this study for comparison purpose.

From Figure 5, it can be noticed that neither the east nor the north can be observed because the former viewing direction is blocked by a container which is at the roof of the building and the latter viewing direction is blocked by other buildings. This is due to the position of the MAX-DOAS instrument relative to other obstacles.

4.7 Differential slant column density

A DOAS measurement require two measurements: the actual measurement and some kind of reference or background measurement which ideally should have as small signal as possible because the difference between these two measurements give the slant column difference. In ground based measurement, there is usually some absorption present in the reference measurement. In this research, a zenith measurement taken at the beginning of the azimuthal scan is used as reference.

$$DSCD_{measured} = SC_{measured} - SC_{reference}$$

Chapter 5

Ancillary Measurements

5.1 Surface In-situ measurements of NO₂ concentrations

The data for the in-situ measurements for the criteria pollutants NO₂ was available from Bremen's air monitoring system (BLUES, 2020) which operates nine air quality monitoring stations. The in-situ monitoring stations collect data over a 24-hour period. Approximately, five of total stations are situated near the industrial and traffic area. The working principle of in-situ instrument is based on chemiluminescence technique, NO (converted from ambient NO₂ using a heated molybdenum converter) oxidizes with excess of ozone in the sample and in-situ analyzer utilizes the chemiluminescence analyzers to detect NO_x and produced chemiluminescence is proportional to available NO in the sample (Lerma et al., 2021). Kattner et. al. (2015) provides the detailed description of the in-situ instrumentation, their operating principles and the calibration procedures.

One of the main aims of this study is to make systematic comparison between the two independent sets i.e., MAX-DOAS path- averaged near surface and in-situ NO₂ VMRs. Basically, the purpose of this comparison is to determine if MAX-DOAS can provide information that will be comparable to data obtained from air quality monitoring stations. A detailed discussion of individual monitoring stations and comparison between two data sets is given in Chapter 6 under section 6.7 and 6.8 respectively.

5.2 Meteorological measurements

Apart from in situ data, Bremen weather station (Deutscher Wetterdienst, 2020) provided data for the meteorological parameters (temperature, pressure, wind speed and wind direction) with a temporal resolution of 10 minutes. The automated weather station is located about 11 km south of the MAX-DOAS measurement site (IUP building, university of Bremen).

Chapter 6

Results and Discussions

This chapter presents the results of the one complete year MAX-DOAS measurements (starting from 01.01.2020 to 31.12.2020) taken on the roof of IUP building in the Bremen. The temporal resolution of MAX-DOAS azimuthal scan varies in winter and summer. During winter, a maximum of 8 complete azimuthal scans can be found per day while a maximum of 20 complete scans is observed per day in summer. The NO₂ DSCDs in 1° elevation angle using zenith direction measurements taken close in time as reference measurements. One of the main aims of this study is to convert the slant column of NO₂ to volume mixing ratio. In order to do that, a series of calculation is performed: correction in temperature, azimuthal correction of NO₂ using H₂O and conversion to mixing ratio using O₄.

6.1 Temperature correction of NO₂ DSCDs

The NO₂ cross section is temperature dependent (both differential and absolute values). The absorption cross section of NO₂ was included in the DOAS fitting technique at a fixed temperature (298 K). This results in an error in the differential slant column of NO₂, which is the ratio of temperature difference between the absorption cross section temperature used in the DOAS fit routine and the absolute temperature of the NO₂ in the troposphere which is presented in Vlemmix et al. (2010). To account for this effect, an estimate of the effective NO₂ temperature correction is required:

$$DSCD_{corrected} = DSCD_{ref} * (1.0 + (T_{actual} - T_{ref}) * 0.00357)$$

where T_{ref} denotes the laboratory temperature at which the NO₂ absorption cross-section was measured. $DSCD_{ref}$ is the differential slant column obtained from the experiment. DOAS fits with NO₂ cross-sections at various temperatures yielded the scaling factor of 0.00357 which has unit of K⁻¹. T_{actual} refers to the interpolated temperature in time obtained from meteorological measurements.

The above temperature corrected equation was applied to all the NO₂ measurements retrieved in the visible spectral region. In figure 6, the NO₂ correction factor applied for whole year using above temperature corrected equation is shown. The correction is of order of several percentage and is larger in winter than in summer.

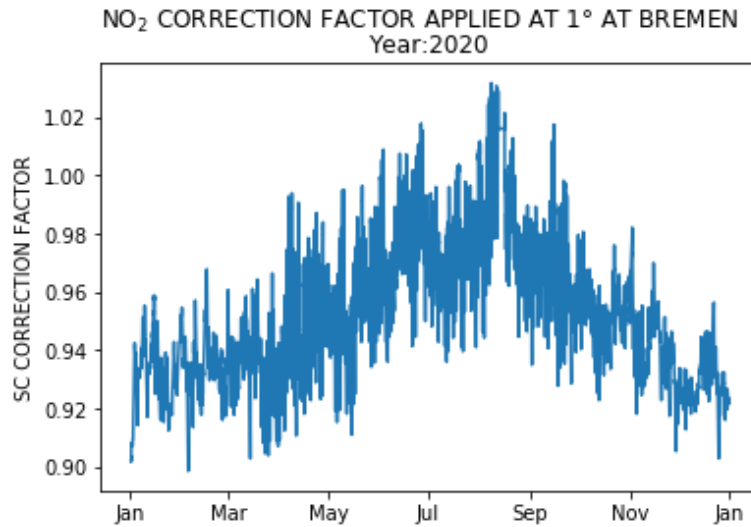


Figure 6. NO₂ correction factor applied using temperature correction.

6.2 Directional correction of NO₂ SCDs

The light coming from the sun is scattered by air molecule (Figure 7) depends on the phase function of the scattering. The phase function explains how strongly the light is scattered in a particular direction. The light path depends on the viewing azimuth because the phase function for scattering (both Rayleigh and Mie) is not spherical but depends on the scattering angle. This causes the light path to change depending on where the sun is located relative to the viewing azimuth directions.

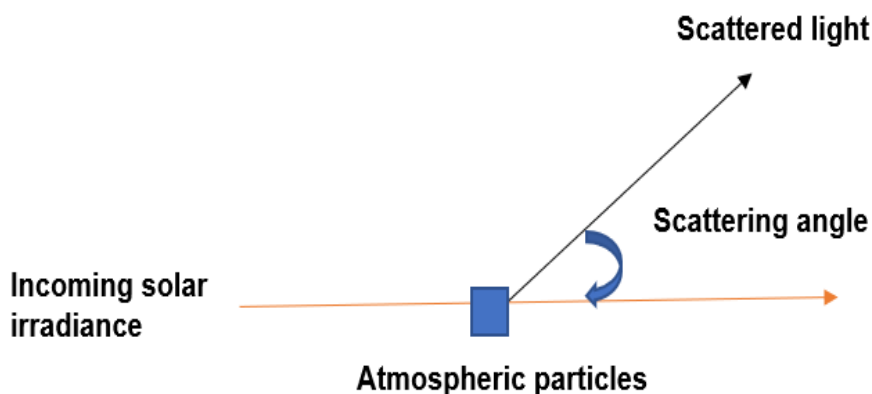


Figure 7. Amount of light scattered with certain angle. This is also called phase function of the aerosols and air molecules. (Adapted from Wikipedia).

The light path is directional dependent which means that atmospheric molecules and particles have the ability to scatter solar radiation in all directions. A total of twenty-four viewing azimuth angles relative to horizon were selected for the instrument and because of the different scattering geometry in each of the angles, correction of azimuthal dependence of light path for NO₂ DSCDs is needed. In principle, the O₄ and H₂O slant column densities can be used to do a first order correction of the NO₂ measurements removing the light path variation with relative azimuth angles. But in this study, O₄ DSCDs are not used for the correction because the vertical distribution of O₄ is not similar to that of NO₂ and therefore the effect of different scattering angles is different for NO₂ and O₄. The basic assumption made for the correction of the azimuthal dependency of the light path length is that H₂O concentrations do not depend on viewing direction. Any variability in the H₂O DSCDs is therefore interpreted as variation in light path length which has to be corrected in the NO₂ measurements.

To attempt a correction of the azimuthal dependency of the light path length, the following process is approached:

- For each azimuthal scan, the measurement direction was determined which had the relative azimuth closest to $\pm 90^\circ$ (for the radiative transfer, positive or negative 90° does not affect the results).

- The H₂O columns for all viewing directions are then divided by those H₂O columns found in 90° relative azimuth direction.
- Finally, the resulting correction factor was then applied to the NO₂ slant columns in each azimuthal scan.

This section involves mainly two steps: In the first step, first order correction of O₄ slant columns using H₂O DSCDs for a single day is presented. In the second step, the azimuthal correction of NO₂ DSCDs is also explained.

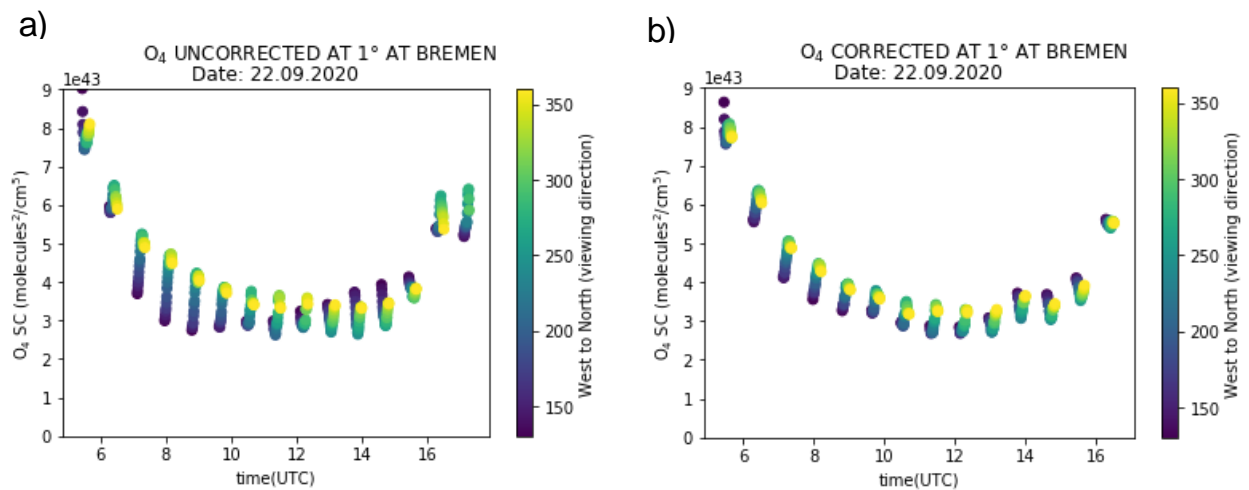


Figure 8. Time series of uncorrected (left panel) and corrected (right panel) O₄ performed for one day.

A single day was chosen to compare the variability of O₄ in the measurements with and without correction. On certain times of the day, around 8 UTC (Figure 8 a)), it can be observed that O₄ measurements are not same in different direction. Since, O₄ slant columns are assumed more or less same in all directions, this must be a light path effect. For O₄ measurements, variation with viewing azimuth is not expected however one can notice it from the figure. So, in order to reduce the angular dependency in O₄ columns the H₂O correction introduced above is applied.

The perfect correction for oxygen dimmer (O₄) would be if the data from all the azimuthal directions superimposed upon each other. This is not the case, but from Figure 8, by comparing the normal and corrected O₄, it is evident that the variation of O₄ slant columns with respect to

azimuth angle has decreased but not disappeared. This is due to two main reasons: firstly, the vertical distribution of O_4 and H_2O are different and secondly, the H_2O is not necessarily distributed homogeneously around the measurement site. Therefore, O_4 has experienced some improvement, assuming that there is no change of H_2O in the direction.

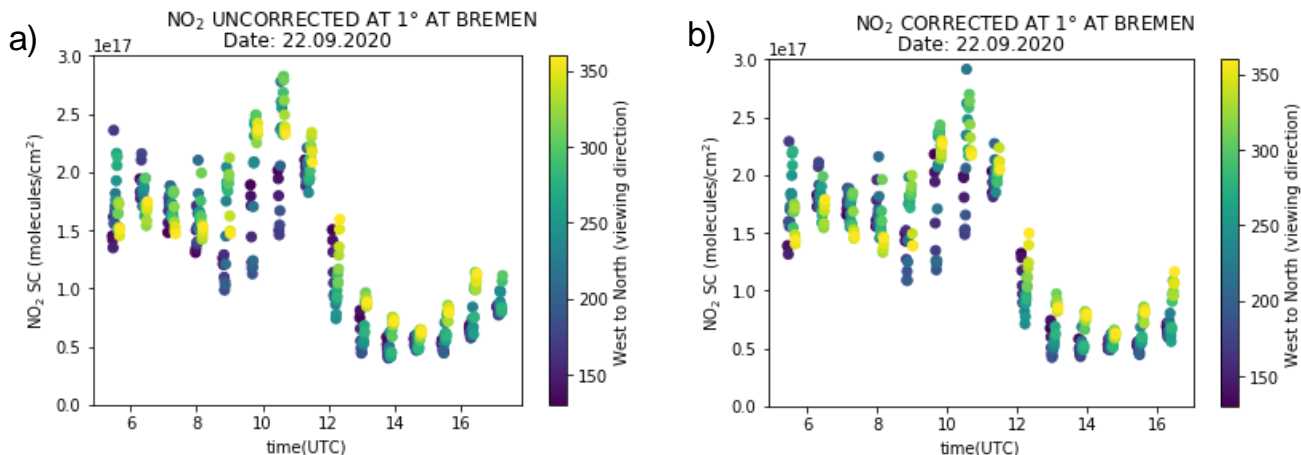


Figure 9. Same as 8 but for NO₂.

Similar to O_4 , the NO_2 data are also not overlapped, and it is not expected because of the local sources of NO_2 close to the ground in the different viewing directions. The corrected NO_2 (Figure 9 b) exhibits a reduction in variability of NO_2 . The variability of NO_2 which means that the variability from the light path is removed and what remains is just the variability in the atmosphere. However, this is not entirely correct since H_2O and NO_2 do not have exactly the same light path. In this sense, what is obtained after the correction is the variability of NO_2 in the atmosphere rather than the variability in the light path. A correction in NO_2 column has been retrieved by employing H_2O DSCDs. The process was repeated for the whole year dataset and obtained a qualitative correction in NO_2 differential slant columns.

6.3 Diurnal and weekend effects

Temporal variability was predicted and observed in the examined results because the observations lasted a year. Study of the diurnal variation of atmospheric trace gases can provide more

information about origins of their emission sources and the chemistry of the atmosphere. The diurnal variation is correlated with emissions, chemical and physical reactions in the boundary layer. Boundary layer generally peaks during noon but decreases in the morning and evening period. The peak of each pollutant is influenced by their lifetimes, physical and chemical behavior (Xu et al., 2021).

Figure 10 shows the hourly averaged diurnal cycles of NO_2 , O_4 and H_2O DSCDs at an elevation angle of 1° . The averaging procedure was introduced separately for weekdays (i.e., Mondays to Fridays) and weekends (i.e., Saturdays and Sundays) in order to examine the difference between them. The time is in the unit of UTC (Coordinated Universal Time) and to convert it to real time zone for Bremen, 2 hours has to be added and this varies depending on daylight saving time. The diurnal profile of NO_2 (Figure 10 a)) columns during weekdays shows higher NO_2 values at around 6 to 7 (UTC) due to morning traffic rush hours. At certain time in the late morning (10 UTC) and early in the afternoon (13 UTC) smooth decrease in slant columns of NO_2 can be observed. The explanation for such behavior can be the higher photolysis rates occur from stronger solar radiance at noon time resulting in lower level of NO_2 (Chan, et al., 2015). Another possible cause around noon can be the concentration of NO_2 over IUP institute is not homogeneously distributed. Thus, the NO_2 distribution is not uniform in all directions and for e.g., if a plume of NO_2 is emitted from the steel factory. Pollutant levels are reduced during the weekend as a result of fewer industrial activities and less traffic volume.

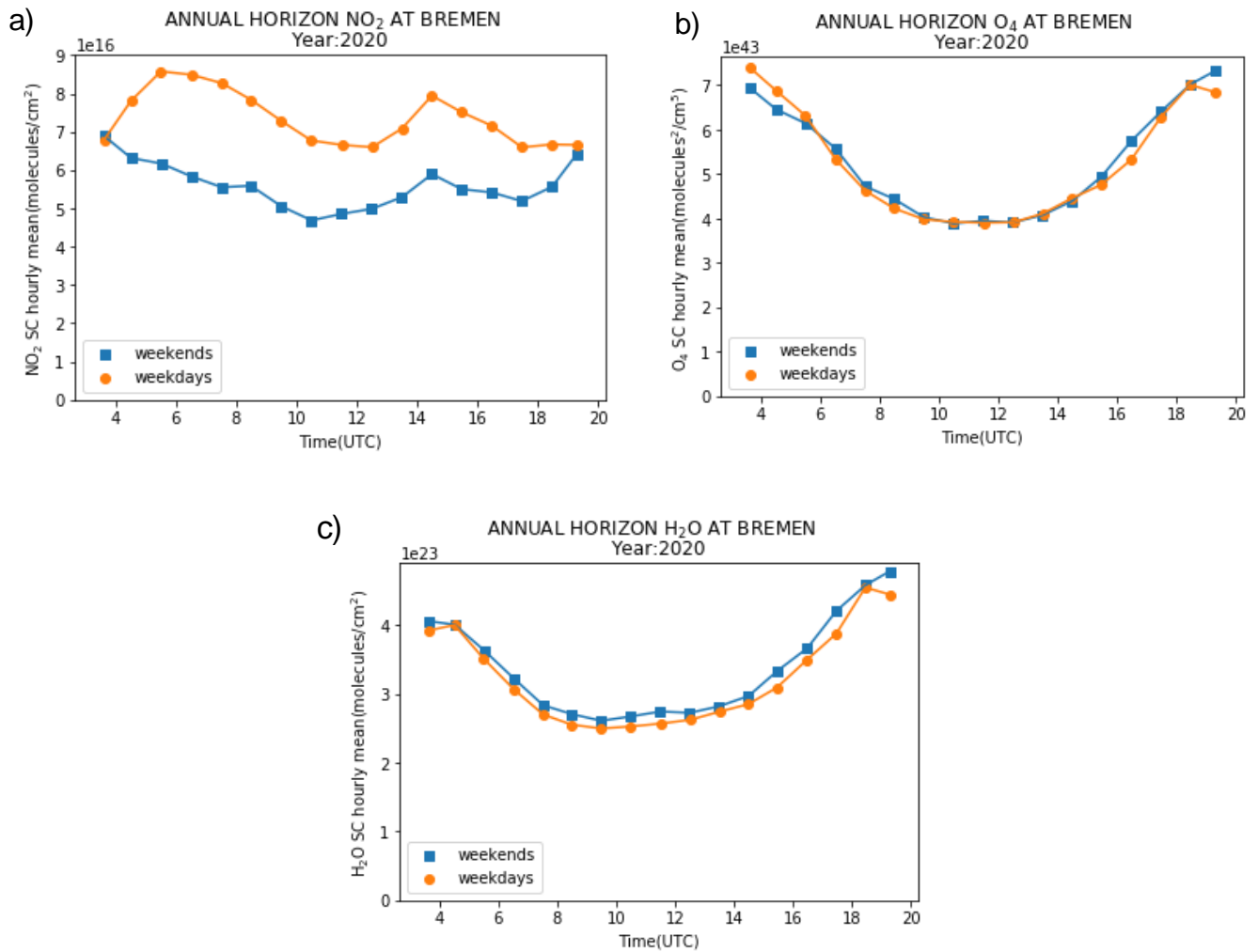


Figure 10. Diurnal variations of slant column densities: a) NO₂, b) O₄, and c) H₂O retrieved in the visible spectral range measured with multiple viewing azimuth angles at 1° elevation angle.

Figure 10 b) illustrates the diurnal variation of O₄ DSCDs which depicts a nice 'U' shape with two DSCDs maxima early morning and late evening. Unlike NO₂, O₄ can never exhibit a large gradient because O₄ is proportional to oxygen. Therefore, what is observed here is equivalent to the change in the light path. There is no difference between weekdays and weekends in O₄ measurements.

It is noticeable that the similar diurnal cycle can be seen in H₂O (Figure 10 c)) compared to O₄ both in weekdays and weekends. Therefore, it is quite interesting to compare water vapor and

oxygen dimmer. One can also notice that there is no weekday and weekend difference in H₂O and this shows that the differences seen in NO₂ are not because of some light path length effect but because of different emission strength. The diurnal pattern can be used to roughly determine at which altitude an absorber is located: A U-shape indicates high altitudes and a more or less constant line indicates close proximity to the surface. Therefore, the figures indicate that NO₂ and H₂O are lower in the atmosphere than O₄.

6.4 Seasonal trends of NO₂, O₄ and H₂O

The seasonal time series analysis (monthly averaged) of measured tropospheric DSCDs of NO₂, O₄ and H₂O for winter (December, January and February), spring (March, April and May), fall (September, October and November) and summer (June, July and August) is shown in figure 11. The tropospheric NO₂ concentrations are higher in the winter and lowest during summer season (Figure 11 a). Maximum NO₂ SC densities during winter are a result of:

- Atmospheric lifetime of NO₂ is longer due to low solar radiance which restricts photochemical processes.
- Use of heating equipment and fossil fuel burning significantly rises and this leads to the elevation of NO₂ levels.
- Lower boundary layer heights due to cooler temperatures which traps the NO₂ near to the surface and lower dispersion efficiency (Ma, et.al, 2013)

Figure 11 b) suggests maximum of O₄ DSCDs are observed during spring season and minimum in winter season. Such low O₄ measurements in winter implies stronger extinction which may indicate a high number of aerosols in the atmosphere.

In contrast to O₄, H₂O concentrations vary with season because of temperature (Figure 13 c)). In addition to that, light path effects play a significant role in the variation of H₂O concentration in the atmosphere.

Clouds have a greater impact on the absorption of tropospheric trace gases such as O₄ and H₂O which are good indicators of increased absorption path lengths caused by multiple Mie scattering within clouds (Meena, et al., 2007).

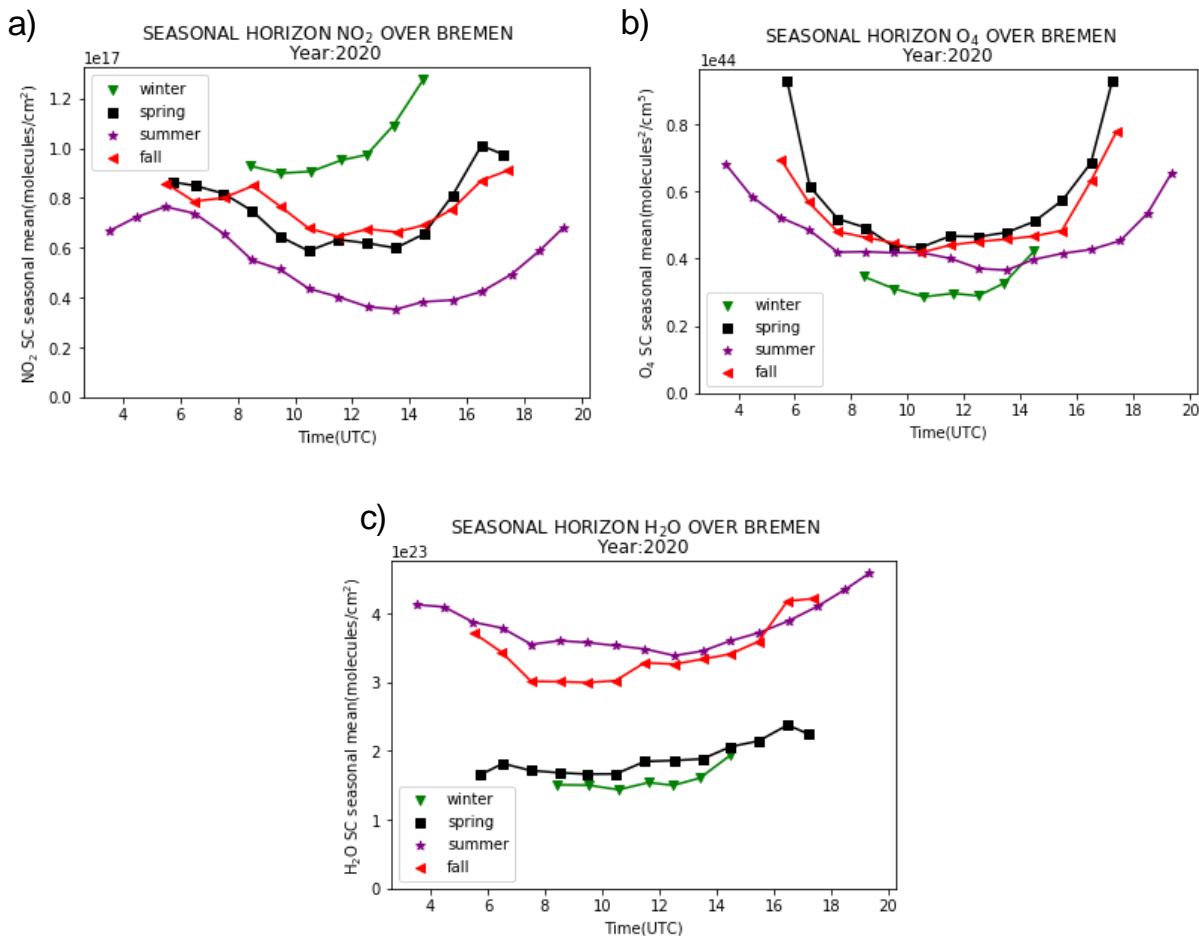


Figure 11. Seasonally averaged diurnal variation of tropospheric a) NO₂ b) O₄ and c) H₂O DSCDs.

6.5 Retrieval of path averaged near surface VMRs from MAXDOAS SCDs

Deployed MAX-DOAS instrument has a lowest usable elevation angle of 1° which allows to detect the most near-surface pollutants with highest sensitivity. Around the measurement site, the highest slant columns are typically measured at this elevation. The MAX-DOAS trace gas column density (equation 3) is the product of the number density of an absorber integrated along the light path through the atmosphere. Differential slant column densities at different viewing azimuth angles are difficult to apply to the estimation of NO₂ concentrations since they comprise not only the concentrations of the trace gases but also light path distributions (Yang et al, 2019). The length of the light path must be known before switching from column density to volume mixing ratio (VMR). Simple geometric approximation (conversion of slant column to vertical column and air mass

factor) is used to estimate the light path length in the troposphere for the high elevation angles like 15°, 20° and so on. However, for the relatively small elevation angle like 1° (used in this research) such approximation fails. In such circumstances, another conversion approach as described in Schreier et al., 2020, is used in order to make a qualitative conversion from slant column to VMR of NO₂. The conversion process involves a total of four steps. In the first step number density of air was calculated using ideal gas equation:

$$n_{air} = \frac{p_{air}}{kT_{air}}$$

with P_{air} and T_{air} are the pressure (unit: Pa) and temperature (unit: K) respectively and k is the Boltzmann constant (unit: JK⁻¹).

Secondly, the number density of O₄ with unit (molecules per volume) was estimated with the equation:

$$n_{O_4} = (n_{O_2})^2 * K_{O_4} = (0.2 * n_{air})^2 * K_{O_4}$$

K_{O_4} is the equilibrium constant of O₄ with unit (volume molecules⁻¹) and this constant is included in the cross section of O₄.

In third step, the length of the light path (unit: length) is estimated with O₄ DSCDs measurements and given as:

$$L = \frac{DSCD_{O_4}}{n_{O_4}}$$

Lastly VMR_{NO_2} with unit parts per billion (ppb) is calculated by applying the following equation:

$$VMR_{NO_2} = \frac{DSCD_{NO_2}}{L * n_{air}}$$

with $DSCD_{NO_2}$ and $DSCD_{O_4}$ being the measured SCDs for NO₂ and O₄, respectively.

Some studies (Sinreich et al., 2013, Wang et al., 2014) focused on the correction factor from radiative transfer calculations for dealing with errors associated with conversion process because of different vertical profile of exponentially decreasing O₄ DSCDs with height and NO₂

layers. In this study, correction factors and systematic errors resulting from the conversion approach are not considered but above-mentioned study explains those factors in detail. The differences in vertical profile of O_4 slant columns contradicts the basic assumption that O_4 is a good proxy for the light path. Resulting near surface VMRs will therefore not reflect the quantity of trace gases at the surface but an average over a certain height in the boundary layer (Seyler et al., 2017).

6.6 Azimuthal dependence of path averaged NO_2 VMR

The seasonally averaged path averaged NO_2 VMR as a function of viewing direction is shown in the figure 12. Higher values of occur during winter whereas lower values occurred during summer season. It is possible that a longer lifetime for NO_2 and lower mixing height during that season (winter) are the main factor. In addition to this, domestic heating also contributes in the elevation of NO_2 VMR in the atmosphere. The NO_2 VMR is averaged as a function of viewing azimuth angle and it is evident that largest values of the respective trace gas volume are obtained when the instrument is pointing towards the city center and railway stations (located at south). During winter season, the maximum value of path averaged NO_2 VMR is approximately 4 ppb and that of summer is around 1.6 ppb.

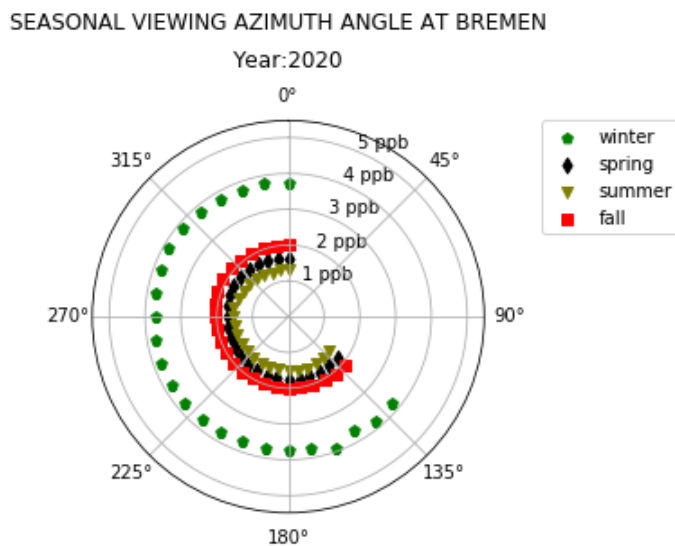


Figure 12. Annual mean NO_2 VMR as a function of viewing direction separated by seasons.

6.7 Variation of In-situ NO₂ measurements over different stations of Bremen

A simple conversion method (1 ppb = 1.88 µg/m³) was applied to convert in-situ NO₂ concentration to in-situ NO₂ VMR. In this section, a detailed description of in-situ data from air quality monitoring stations (BLUES site) is given. These measurements are mainly used in the analysis with the aim of comparison with MAX-DOAS measurements. MAX-DOAS can only collect measurements during daylight hours while in-situ instruments are able to take measurements during night too. The detailed description of individual station is taken from BLUES, 2007. Table 1 shows the atmospheric species measured by these monitoring stations.

Name of the stations	Measured species
Bremen Mitte	O ₃ , SO ₂ , NO _x , CO, PM ₁₀
Bremen Nord	SO ₂ , NO _x , PM ₁₀ , O ₃
Bremen Ost	SO ₂ , NO _x , PM ₁₀ , O ₃ , PM _{2.5}
Bremen Oslebhausen	SO ₂ , NO _x , CO, PM ₁₀
Bremen Hasenbüren	SO ₂ , NO _x , PM ₁₀ , O ₃ , PM _{2.5} , meteorological parameter
Bremerhaven Hansestraße	CO, SO ₂ , NO _x , PM ₁₀ , O ₃ , PM _{2.5} , meteorological parameter
Verkehr 1	NO _x , CO, PM ₁₀ , meteorological parameters
Verkehr 4	NO _x , PM ₁₀
Verkehr 5	NO _x , CO, PM ₁₀ , meteorological parameters

Table 1: Atmospheric species measured by Bremen air quality monitoring stations. Meteorological parameters include temperature, relative humidity, wind speed and wind direction. (BLUES, 2017)

Verkehr 1, Verkehr 4 and Verkehr 5

These three monitoring stations are specially in the traffic area with the traffic volume of more than 20,000 vehicles / day. Figure 13 a), b) and c) are the measurements of NO₂ VMR in these three stations and suggest that near surface NO₂ VMR is higher during fall and spring season.

Bremen Nord

This station is located on the premises of the Bremen-Nord fire station. To the west, the station is slightly shielded by a two-storey building and B74 highway is situated to the south of the station at a distance of 300 m. In the immediate vicinity, there is predominantly small businesses and multi storey buildings.

Bremen Mitte

Within the radius of 1000m from the station, there are multi-storey residential buildings, businesses and predominantly a parking lot.

Bremen Hasenbüren

To the south of this station, industrial area is situated with numerous industrial emission sources. Figure 16 c shows the industrial NO₂ VMR mostly during fall season.

Bremen Ost

Residential Buildings and a large automobile plant are located within the radius of 1 km.

Bremen Oslebhausen

The station is within the residential area away from traffic emissions but in the sphere of influence of the industrial area in the west at a distance of about 3000m.

Bremerhaven Hansestraße

The station is located in the vicinity of the ports of Bremerhaven. Highest amount of NO₂ volume in the atmosphere can be observed in winter (Figure 14 f)).

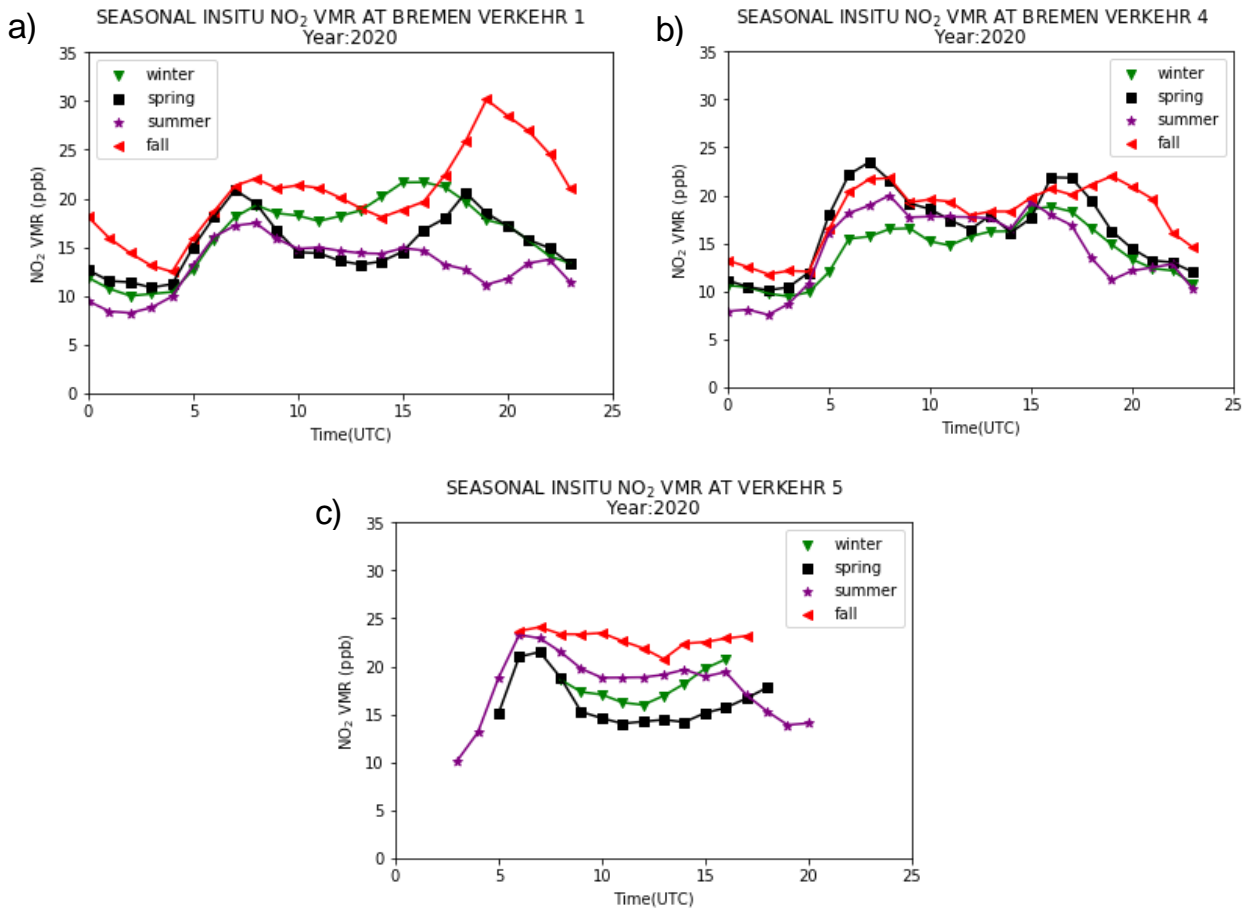


Figure 13. In-situ measurements of NO₂ VMR measured near the traffic area separated by seasons.

Because the station's location is around residential area, extremely large values of NO₂ cannot be observed in figure 14 a), b) c) and d) however results show that at all stations winter values are greater than those of other seasons and this is different from the traffic stations.

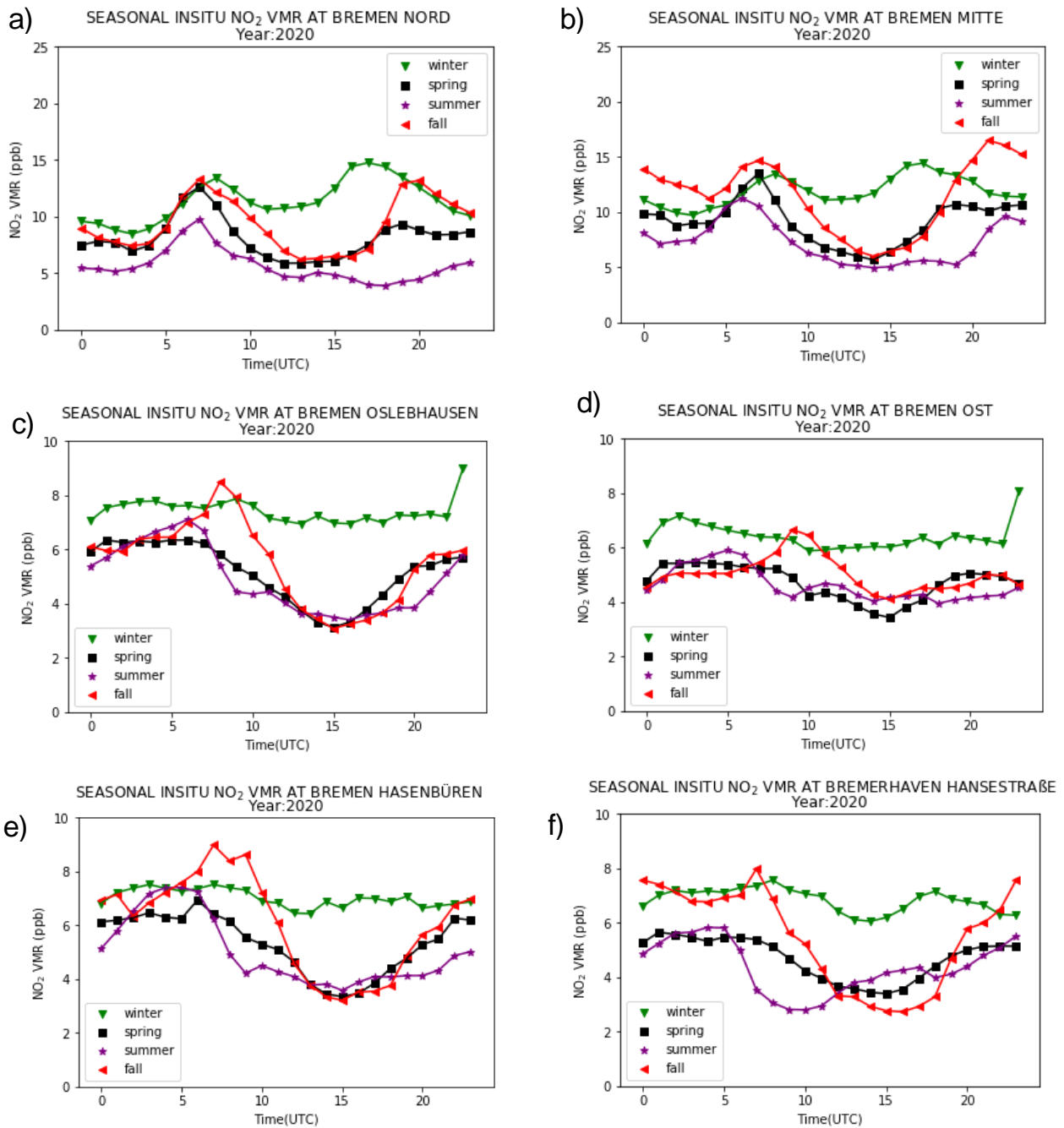


Figure 14. Same as 13 but near for residential a), b) c), d) and industrial e) and port f).

6.8 Comparison of MAX-DOAS data with In-situ measurements

During MAX-DOAS measurements, an extended light path through the atmosphere is probed, while in-situ trace gas analyzers measure concentration at the site of the instrumentation. The measurements from in-situ data were analyzed for the same time period as of MAX-DOAS and are used for making systematic comparison with MAX-DOAS data. It is difficult, however to compare the data from in-situ instrument with those from MAX-DOAS instrument due to their significantly different air volumes (Heckel et al., 2005). A comparison of the in-situ and MAX-DOAS temporal mean is demonstrated in figure 15.

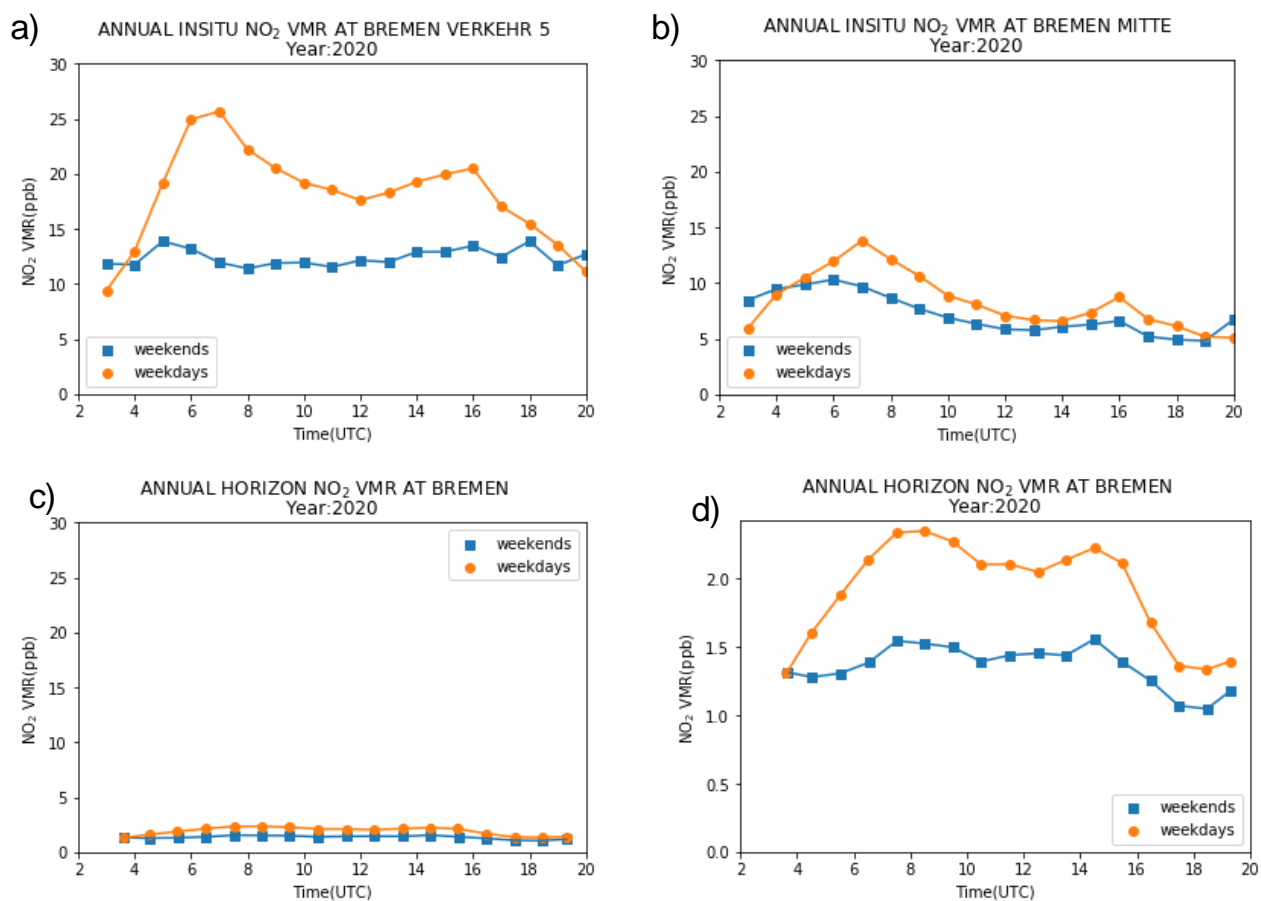


Figure 15. Averaged NO₂ VMR observed by a) in-situ over traffic regions) and b) in-situ over countryside and c) MAX-DOAS with adapted y-axis d) MAX- DOAS with normal y- axis.

An exact agreement cannot be expected between the trace gas measurements of both instrument due to the differences in the measurement volumes. Figure 15 a) shows the diurnal variation of traffic influenced NO_2 measurements with enhanced values in the morning and evening time during the rush hour. Comparison between figure 15 b) and c) would be fair since the MAX-DOAS instrument is situated in the residential area. However, figure 15 b) illustrates maximum NO_2 VMR of about 14 ppb and 10 ppb during weekdays and weekend respectively while horizon measurements are significantly lower since the instrument is situated in cleaner area and both instruments observe different air masses. In-situ measurements of NO_2 VMR are substantially higher than horizon observations, however diurnal variability seems to agree very well. In fact, the diurnal variation and the weekday / weekend variation is more similar to the traffic station than to the residential measurements.

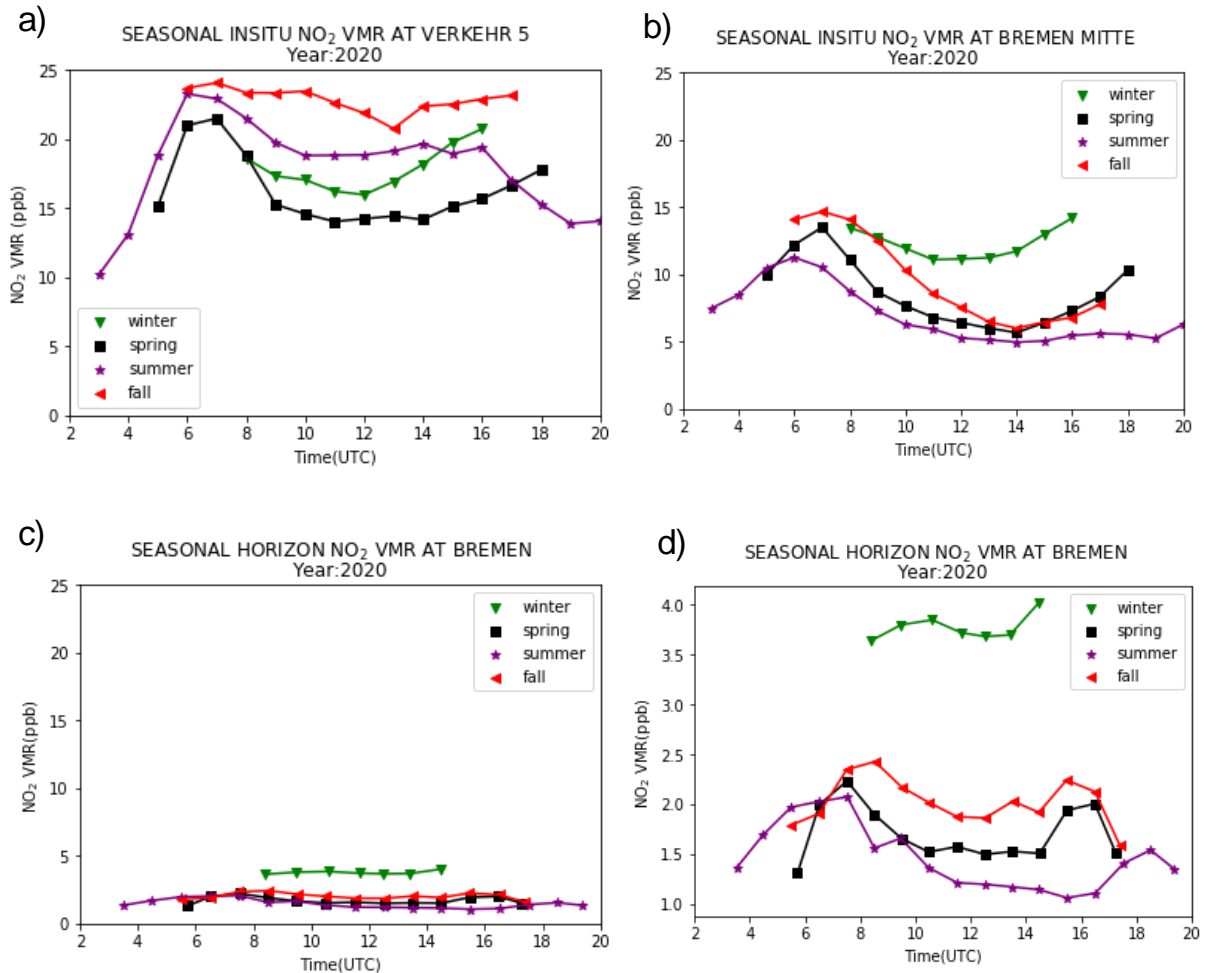


Figure 16: Same as 15 but separated by the seasons.

Figure 16 a) shows highest (lowest) NO₂ VMR during fall (spring) in areas of heavy traffic volume. Similarly, higher winter values and lowest summer values can be observed in figure 16 b) and c). The reason for this is that air quality stations measure near surface NO₂ whereas MAX-DOAS measures over the boundary layer. For the seasonality, the relative magnitudes appear to match better to the residential in-situ station with the exception of winter, where the MAX-DOAS values are suspiciously high, possibly because of the relatively large solar zenith angle which reduces the sensitivity to the surface layer and may create problems with the O₄ correction.

Results from MAX-DOAS and ground based in-situ instrument differ in systematic ways possibly because of the missing correction factors originating from the atmospheric profile of air pollutants such as NO₂ and O₄ leading to an inconsistent difference of NO₂ VMR (Seyler, 2020).

6.9 Dependence of NO₂ pollution levels on meteorological parameters

Several factors play a significant role in determining the chemical composition of the lower atmosphere including meteorology since it deeply influences how long trace gases stay in the atmosphere (Tanvir et al., 2021). In order to evaluate the dependency of tropospheric NO₂ pollutant on wind speed and wind direction, the parameters are first linearly interpolated with respect to time. Then the data is divided into 8 bins of 45°; the center of the bin is set as North being 0° moving in clockwise direction.

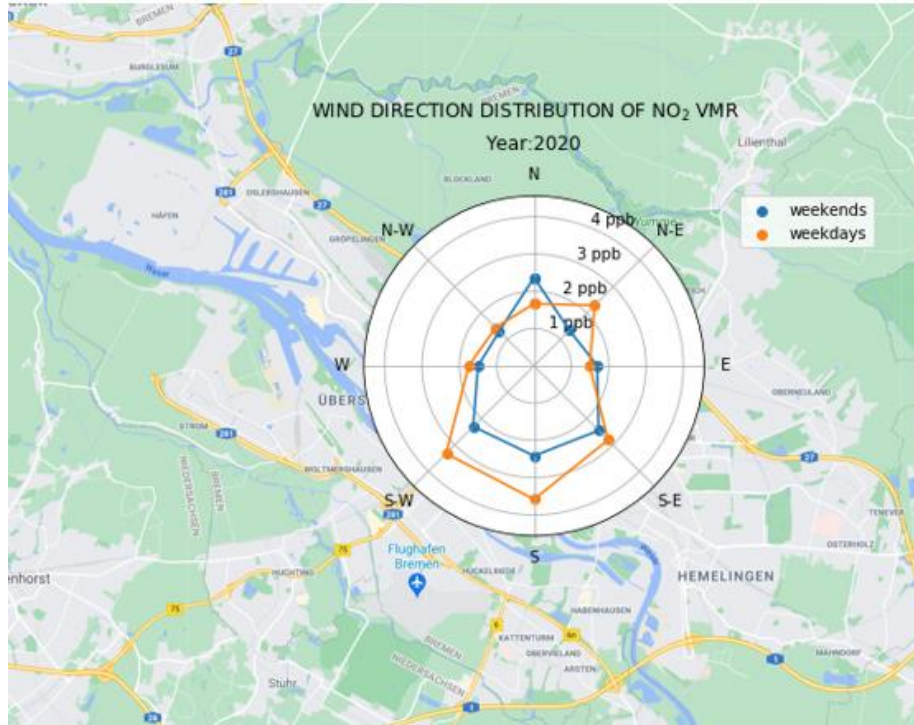


Figure 17. Dependence of MAX-DOAS NO₂ mixing ratios on wind direction separated by weekdays and weekends around measurement site.

The averaged NO₂ VMR for each wind direction is shown in the figure 17. The tropospheric NO₂ VMR will be dependent on the wind direction because NO_x emission sources are not homogeneously distributed around the measurement site. As observed from the figure, the NO₂ amounts are higher during weekdays and weekends when the wind blows from the south and south-west direction. This higher amount of NO₂ is largely controlled by the traffic coming from city center which is situated in the south-west direction. The air masses of NO₂ content blowing from all other directions are probably due to the land-based sources and some other anthropogenic emissions. In addition to this one can also say that the difference between weekdays and weekends is much larger when the wind is blowing from the city. The above figure also depicts the strongest relative decrease in the direction from west to north.

The NO₂ amount is investigated for two different conditions: wind from south and wind from north. The results obtained from those conditions for NO₂ VMR is presented in the left and right panel of Figure 18. The objective behind doing this is to show the dependency of NO₂ amount with wind direction from the source region and background region. The horizontally path averaged NO₂ volume mixing ratio increases slightly reaching highest around 3.7 ppb (5 m/s) (see left panel) and

reaches to the minimum with increasing speed. Such enhanced NO₂ values can be due to the anthropogenic sources especially from the city center. In contrast to that, NO₂ amount has highest volume of approximately 2.1 ppb at around 1m/s speed (see right panel). A possible explanation for an apparent increase in NO₂ mixing ratio at lower speeds can be that if there is very little wind then may be wind from the pollution in the city is not blown to the instrument.

In general, both cases (Figure 18) have shown reduction in NO₂ pollution level with higher wind speeds. Higher wind speed favors the dispersion of NO₂ pollutant, which cleans the air. Vlemmix et., al. (2015), observed a strong decrease with increasing speeds due to local sources in De Bilt, Netherlands.

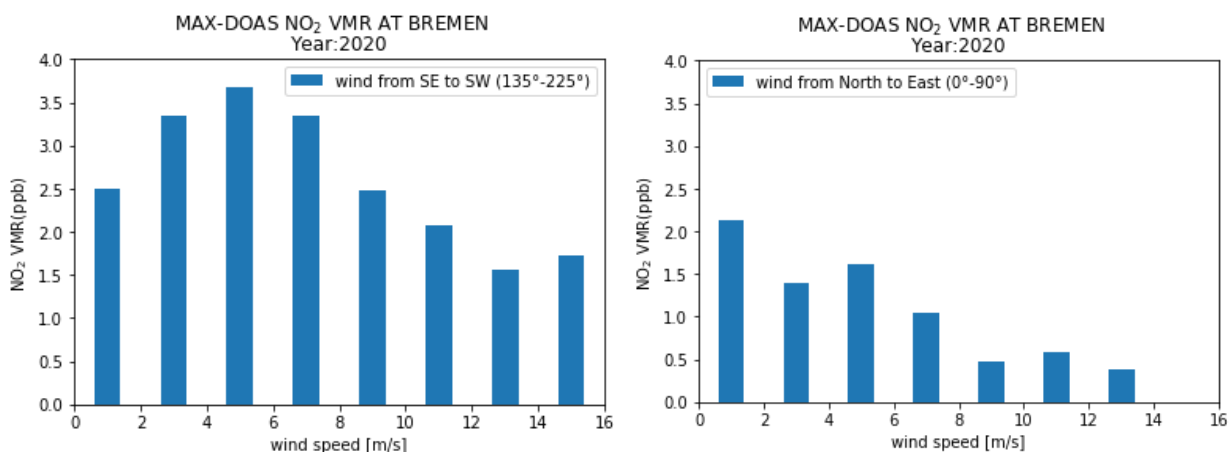


Figure 18. Path averaged tropospheric NO₂ VMR as a function of windspeed. The left and right panels show the wind direction from south east to south west and north to east respectively.

Chapter 7

Summary and Conclusions

This thesis focuses on investigating the horizontal variability of tropospheric NO₂. The measurements used in this study are the continuous daytime spectral measurements in the visible spectral range over a period of one year at the preferred azimuth viewing direction (total 24) at an elevation angle of 1° and the instrument deployed for this research is Multi Axis Differential Optical Absorption Spectroscopy (MAX-DOAS).

Measurements and analysis of slant columns

Before presenting the results, some corrections are performed in order to obtain correct NO₂ volume mixing ratios. The first analysis in this step is temperature correction. The absorption cross section of NO₂ is temperature dependent. During the DOAS fitting process this was accounted and therefore NO₂ columns determined is not correct. A temperature correction equation is used to get correct time series of NO₂ DSCDs. Secondly, azimuthal correction of NO₂ slant columns is evaluated. Because of the scattering geometry in 24 individual viewing azimuth direction, a correction in each of the direction is needed. The correction is obtained by employing H₂O columns which is under positive or negative 90° relative azimuth angle. For NO₂, the correction is to extract the part coming from different concentrations by removing the part coming from differences in light path. However, a perfect correction could not be achieved but at least some improvements were observed after applying the correction.

In addition to MAX-DOAS retrievals some ancillary measurements i.e., in-situ and meteorological data were used during the analysis. The in-situ measurements are used to make systematic comparison between path-averaged NO₂ VMR and near surface NO₂ VMR.

Trace gas distributions in Bremen

An average diurnal variation of NO₂ slant column is studied for the week days and weekends. The results show higher level of NO₂ emission during the weekdays. An explanation for such results can be anthropogenic activities mainly traffic density and industrial activities. Also, the temporal variation of O₄ and H₂O is analyzed. Both trace gases depicted a nice U shape profile with two maxima early in the morning and late in the evening. In addition to that, no significant differences during the day are observed in both trace gases between weekdays and weekends. The seasonal

variability of averaged NO₂ is investigated on the basis of four seasons: winter (DJF), summer (JJA), fall (SON) and spring (MAM). As expected, winter season holds maximum of NO₂ concentration while summer has the minimum. The tropospheric NO₂ during winter stays longer in the atmosphere because of the less photochemical reactions and shallower boundary layer height leads to the increase in NO₂ amount.

After analyzing differential slant column density of all three atmospheric trace gases, a smooth switch is made from slant column to volume mixing ratio (VMR) of NO₂. For doing so, a conversion method has been introduced because of the lowest elevation angle used in this research. O₄ slant columns is used in the conversion process for calculating length of the light path. The slant column is finally converted to VMR with the aid of some calculations. The horizontal variability of NO₂ is determined from an analysis of azimuthal dependence. Seasonally averaged NO₂ VMR obtained by deploying MAX-DOAS instrument in different viewing direction indicates lower (higher) amount of NO₂ in summer (winter).

A detailed description of in-situ measurements has been presented to see the variation of in-situ NO₂ over different monitoring stations. Some of the monitoring stations are situated near the traffic region while others are more near to the residential areas. In-situ measurements are mainly used in this study to make a systematic comparison with the horizon measurements. MAX-DOAS results were compared with those monitoring stations where the impact of traffic area is low. Since, perfect agreement is not expected while comparing two independent sets because MAX-DOAS instrument is situated in more cleaner areas. Hence, a systematic comparison is achieved however, MAX-DOAS measurements were lower in magnitude as compared to other monitoring stations.

Finally, the dependency of path averaged NO₂ VMR on meteorological parameters; wind direction and wind speed are studied. Wind direction are divided into two conditions in order to see the dependency of NO₂ VMR with direction from source and background region. The NO₂ VMR is higher when the wind blows from the south and south-west direction (city-center is situated in this direction) carrying traffic dominated NO₂. The effect of the wind speed is low on NO₂ VMR when the wind is blowing from the north rather bringing clear air to the measurement site.

Outlook

For further research, the following analyses appear to be of interest. As described in Section 5.5, the results of converting NO_2 DSCDs to VMR, are subject to some errors due to the vertical profile of the O_4 slant column. Thus, a correction factor can be introduced to compensate for such errors. Furthermore, concentration of air pollutants has decreased significantly due to the Covid-19 lockdown measures. Therefore, a qualitative comparison between the data during and before the lockdown would lead to an interesting result.

References

Blechschmidt, A.M., Arteta, J., Coman, A., Curier, L., Eskes, H., Foret, G., Gielen, G., Hendrick, F., Marécal, V., Meleux, F., Parmentier, J., Peters, E., Pinardi, G., Piters, A.J.M., Plu, M., Richter, A., Segers, A., Sofiev, M., Valdebenito, A.M., Roozendael, M.V., Vira, J., Vlemmix, T. and Burrows, J.P.: Comparison of tropospheric NO₂ columns from MAX-DOAS retrievals and regional air quality model simulations, *Atmos. Chem. Phys.*, 20, 2795-2823, <https://doi.org/10.5194/acp-20-2795-2020>, 2020.

BLUES - Das Bremer Luftüberwachungssystem, URL: <https://www.bremerhaven.de/sixcms/media.php/94/a2-jahresbericht2007.pdf>, visited on: 01.10.2020, 2007.

BLUES - Das Bremer Luftüberwachungssystem , URL: <https://www.bauumwelt.bremen.de/umwelt/luft/luftqualitaet-24505>, visited on: 01.10.2020, 2017.

BLUES - Das Bremer Luftüberwachungssystem, URL: <https://luftmessnetz.bremen.de/lqi>, visited on: 06.06.2020, 2020.

Bösch, T.: Detailed analysis of MAX-DOAS measurements in Bremen: Spatial and temporal distribution of aerosols, formaldehyde and nitrogen dioxide, 2018.

Chan, K.L., Hartl, A., Lam, Y.F., Xie, P.H., Liu, W.Q., Cheung, H.M., Lampel, J., Pöhler, D., Li, A., Xu, J., Zhou, H.J., Ning, Z. and Wenig, M.O.: Observations of tropospheric NO₂ using ground based MAX-DOAS and OMI measurements during the Shanghai World Expo 2010, *Atmospheric environment*, 119, 45-58, <https://doi.org/10.1016/j.atmosenv.2015.08.041>, 2015.

Chan, K. L., Wiegner, M., Geffen, J.V., Smedt, I.D., Alberti, C., Cheng, Z., Ye, S. and Wenig, M.O.: MAX-DOAS measurements of tropospheric NO₂ and HCHO in Munich and the comparison to OMI and TROPOMI satellite observations. *Atmospheric Measurement Techniques*, 13, 4499–4520, <https://doi.org/10.5194/amt-13-4499-2020>, 2020.

DWD- Deutscher Wetterdienst, URL: https://opendata.dwd.de/climate_environment/CDC/observations_germany/climate/, 2020.

Finlayson-Pitts, B.J., Pitts, J.N., *Chemistry of the upper and lower atmosphere*, Academic Press, New York, 3-8, 2000.

Georgoulias, A. K., van der A, R. J., Stammes, P., Boersma, K. F., and Eskes, H. J.: Trends and trend reversal detection in 2 decades of tropospheric NO₂ satellite observations, *Atmos. Chem. Phys.*, 19, 6269–6294, <https://doi.org/10.5194/acp-19-6269-2019>, 2019.

Gratsea, M., Vrekoussis, M., Richter, A., Wittrock, F., Schönhardt, A., Burrows, J., Kazadzis, S., Mihalopoulos, N. and Gerasopoulos, E.: Slant column MAX-DOAS measurements of nitrogen dioxide, formaldehyde, glyoxal and oxygen dimer in the urban environment of Athens, *Atmospheric Environment*, 135, 118-131, <https://doi.org/10.1016/j.atmosenv.2016.03.048>, 2016.

Heckel, A., Richter, A., Tarsu, T., Wittrock, F., Hak, C., Pundt, I., Junkermann, W. and Burrows, J.P.: MAX-DOAS measurements of formaldehyde in the Po-Valley, *Atmos. Chem. Phys.*, 5, 909–918, 2005.

Hönninger, G., Friedeburg C.V. and Platt, U.: Multi- Axis Differential Optical Absorption Spectroscopy (MAX-DOAS), *Atmos. Chem. Phys.*, 4, 231–254, 2004.

Irie, H., Takashima, H., Kanaya, Y., Boersma, K. F., Gast, L., Wittrock, F., Brunner, D., Zhou, Y., and Van Roozendaal, M.: Eight-component retrievals from ground-based MAX-DOAS observations, *Atmos. Meas. Tech.*, 4, 1027–1044, <https://doi.org/10.5194/amt-4-1027-2011>, 2011.

Kattner, L., Mathieu-Üffing, B., Burrows, J.P., Richter, A., Schmolke, S., Seyler, A. and Wittrock, F.: Monitoring compliance with sulfur content regulations of shipping fuel by in situ measurements of ship emissions, *Atmos. Chem. Phys.*, 15, 10087–10092, [doi:10.5194/acp-15-10087-2015](https://doi.org/10.5194/acp-15-10087-2015), 2015.

Lerma, Z. O., Cardenas, C. R., Friedrich, M.M., Stremme, W., Bezanilla, A., Arellano, E.J. and Grutter, M.: Evaluation of OMI NO₂ Vertical Columns Using MAX-DOAS Observations over Mexico City. *Remote Sens.*, 13, 761, <https://doi.org/10.3390/rs13040761>, 2021.

Ma, J.Z., Beirle, S., Jin, J.L., Shaiganfar, R., Yan, P. and Wagner T.: Tropospheric NO₂ vertical column densities over Beijing: results of the first three years of ground-based MAX-DOAS measurements (2008- 2011) and satellite validation, *Atmos. Chem. Phys.*, 13, 1547–1567, [doi:10.5194/acp-13-1547-2013](https://doi.org/10.5194/acp-13-1547-2013), 2013

Meena, G.S. and Jadhav D.B.: Study of diurnal and seasonal variation of atmospheric NO₂, O₃, H₂O and O₄ at Pune, India, *Atmósfera*, 20(3), 271-287, 2007.

Mie, G.: Beiträge zur optik trüber medien, speziell kolloidaler metallösungen, *Ann. physik*, 25, 377, <https://doi.org/10.1002/andp.19083300302>, 1908.

Platt, U., Perner, D. and Pätz, H.: Simultaneous measurement of atmospheric CH₂O, O₃, and NO₂ by differential optical absorption. *J. Geophys. Res.* 84, 6329–6335, 1979.

Platt, U.: Differential optical absorption spectroscopy (DOAS), in *Air Monitoring by Spectroscopic Techniques*, Chem. Anal. Ser., edited by Sigrist, M. W., 127, 27–84, John Wiley, New York, 1994.

Platt, U. and Stutz, J.: *Differential Optical Absorption Spectroscopy*, Springer-Verlag Berlin Heidelberg, 137-139, 2008.

Rasmussen, R.A. and Khalil, M.A.K.: The behavior of trace gases in the troposphere, *The Science of the Total Environment*, 48, 169-186, [https://doi.org/10.1016/S0048-9697\(86\)80003-1](https://doi.org/10.1016/S0048-9697(86)80003-1), 1985.

Richter, A.: Nitrogen oxides in the troposphere – What have we learned from satellite measurements?, *The European Physical Journal Conference*, DOI: 10.1140/epjconf/e2009-00916-9, 2009.

Schreier, S. F., Richter, A., Peters, E., Ostendorf, M., Schmalwieser, A. W., Weihs, P., and Burrows, J.P.: Dual ground-based MAX-DOAS observations in Vienna, Austria: Evaluation of horizontal and temporal NO₂, HCHO, and CHOCHO distributions and comparison with independent data sets, *Atmospheric Environment: X*, 5, 10059, <https://doi.org/10.1016/j.aeaoa.2019.100059>, 2020.

Sinreich, R., Merten, A., Molina, L., and Volkamer, R.: Parameterizing radiative transfer to convert MAX-DOAS DSCDs into near-surface box-averaged mixing ratios, *Atmos. Meas. Tech.*, 6, 1521–1532, doi:10.5194/amt-6-1521-2013, 2013.

Seyler, A., Wittrock, F., Kattner, L., Mathieu-Üffing, B., Peters, E., Richter, A., Schmolke, S., and Burrows, J.P.: Monitoring shipping emissions in the German Bight using MAX-DOAS measurements, *Atmos. Chem. Phys.*, 17, 10997–11023, <https://doi.org/10.5194/acp-17-10997-2017>, 2017.

Seyler, A.: Investigating air quality in the marine environment of the North and Baltic Sea with MAX-DOAS measurements, 2020.

Smedt, I.D., Pinardi, G., Vigouroux, C., Compemolle, S., Bais, A., Benavent, N., Boersma, F., Chan, K.L., Donner, S., Eichmann, K.U., Hedelt, P., Hendrick, F., Irie, H., Kumar, V., Lambert, J.C., Langerock, B., Lerot, C., Liu, C., Loyola, D., Pöters, A., Richter, A., Cárdenas, C.R., Romahn, F., Ryan, R.G., Sinha, V., Theys, N., Vlietinck, J., Wagner, T., Wang, T., Yu, H. and Roozaendel, M.V.: Comparative assessment of TROPOMI and OMI formaldehyde observations and validation against MAX-DOAS network column measurements, *Atmos. Chem. Phys.*, 21, 12561–12593, <https://doi.org/10.5194/acp-21-12561-2021>, 2021.

Sweigart, A.V.: Radiative transfer in atmospheres scattering according to the Rayleigh phase function with absorption, *The Astrophysical Journal Supplement Series No. 182*, 22:1-80, 1969.

Tan, W., Zhao, S., Liu, C., Chan, K.L., Xie, Z., Zhu, Y., Su, W., Zhang, C., Liu, H., Xing, C. and Liu, J.: Estimation of winter time NO_x emissions in Hefei, a typical inland city of China, using mobile MAX-DOAS observations, *Atmospheric Environment*, 200, 228-242, <https://doi.org/10.1016/j.atmosenv.2018.12.009>, 2019.

Tanvir, A., Javed, Z., Jian, Z., Zhang, S., Bilal, M., Xue, R., Wang, S. and Bin, Z.: Ground-Based MAX-DOAS Observations of Tropospheric NO₂ and HCHO During COVID-19 Lockdown and Spring Festival Over Shanghai, China. *Remote Sens.* 2021, 13, 488. <https://doi.org/10.3390/rs13030488>, 2021.

The Federal Environment Agency, last updated: 07/03/2020, URL: <https://www.umweltbundesamt.de/daten/luft/luftschadstoff-emissionen-in-deutschland/stickstoffoxid-emissionen#entwicklung-seit-1990>.

Vandaele, A. C., Fayt, C., Hendrick, F., Hermans, C., Humbled, F., van Roozendaal, M., Gil, M., Navarro, M., Puentedura, O., Yela, M., Braathen, G., Stebel, K., Tørnkvist, K., Johnston,

P., Kreher, K., Goutail, F., Mieville, A., Pommereau, J.-P., Khaikine, S., Richter, A., Oetjen, H., Wittrock, F., Bugarski, S., Frie, U., Pfeilsticker, K., Sinreich, R., Wagner, T., Corlett, G., and Leigh, R.: An intercomparison campaign of ground-based UV-visible measurements of NO₂, BrO, and OCIO slant columns: Methods of analysis and results for NO₂, *J. Geophys. Res.*, 110, 10.1029/2004JD005423, 2005.

Vlemmix, T., Piters, A.J.M., Stammes, P., Wang, P. and Levelt, P.F.: Retrieval of tropospheric NO₂ using the MAX-DOAS method combined with relative intensity measurements for aerosol correction, *Atmos. Meas. Tech.*, 3, 1287–1305, doi:10.5194/amt-3-1287-2010, 2010.

Wagner, T., Chance, K., Freiß, U., Gil, M., Goutail, F., Hönninger, G., Johnston, P.V., Tørnkvist, K. K., Kostadinov, I., Leser, H., Petritoli, A., Richter, A., Roozendael, M.V. and Platt, U.: Correction of the Ring effect and I₀ effect for DOAS observations of scattered sunlight, in: *Proc. of the 1st DOAS Workshop, Heidelberg, Germany, 2001*.

Wang, Y., Li, A., Xie, P. H., Wagner, T., Chen, H., Liu, W.Q. and Liu, J.G.: A rapid method to derive horizontal distributions of trace gases and aerosols near the surface using multi-axis differential optical absorption spectroscopy, *Atmos. Meas. Tech.*, 7, 1663–1680, doi:10.5194/amt-7-1663-2014, 2014.

Wittrock, F., Oetjen, H., Richter, A., Fietkau, S., Medeke, T., Rozanov, A. And Burrows, J.P.: MAX-DOAS measurements of atmospheric trace gases in Ny-Alesund - Radiative transfer studies and their application, *Atmos. Chem. Phys.*, 4, 955–966, 2004.

Wikipedia, Aerosol Phase function Measurements, URL:
http://www.soest.hawaii.edu/porter/AerosolPhase_Function.html, visited on: 04.09.2020.

Xu, S., Wang, S., Xia, M., Lin, H., Xing, C., Ji, X., Su, W., Tan, W., Liu, C. and Hu, Q.: Observations by Ground-Based MAX-DOAS of the Vertical Characters of Winter Pollution and the Influencing Factors of HONO Generation in Shanghai, China. *Remote Sens.* 2021, 13, 3518, <https://doi.org/10.3390/rs13173518>, 2021.

Yang, T., Si, F., Luo, Y., Zhan, K., Wang, P., Zhou, H., Zhao, M. and Liu, W.: Source contribution analysis of tropospheric NO₂ based on two-dimensional MAX-DOAS measurements, *Atmospheric Environment*, 210, 186- 197, <https://doi.org/10.1016/j.atmosenv.2019.04.058>, 2019.

Zhou, B., Yang, S.N., Wang, S.S. and Wagner, T.: Determination of an effective trace gas mixing height by differential optical absorption spectroscopy (DOAS), *Atmos. Meas. Tech.*,2, 1663–1692, 2009.